ADDIS ABABA UNIVERSITY
ADDIS ABABA INSTITUTE OF TECHNOLOGY
SCHOOL OF ELECTRICAL AND COMPUTER ENGINEERING

Design of Integrated Guidance and Control for a Missile using Sliding Mode Control Technique

A thesis Submitted to the School of Electrical and Computer Engineering of Addis Ababa Institute of Technology, School of Graduate Studies, Addis Ababa University, In partial fulfillment of the Requirement for the Degree of Masters of Science in Control Engineering

By
Addisalem Hailegnaw

Advisor: Dr. Dereje Shiferaw

October, 2019
Addis Ababa, Ethiopia

ADDIS ABABA UNIVERSITY
ADDIS ABABA INSTITUTE OF TECHNOLOGY
SCHOOL OF ELECTRICAL AND COMPUTER ENGINEERING

Design of Integrated Guidance and Control for a Missile using Sliding Mode Control Technique

By
Addisalem Hailegnaw

APPROVED BY BOARD OF EXAMINERS

______________________	______________
Chairman, Department of Graduate Committee	Signature
Dr. Dereje shiferaw	______________
Advisor	Signature
______________________	______________
Internal Examiner	Signature
______________________	______________
External Examiner	Signature

DECLARATION

I, the undersigned, declare that this thesis is my original work, has not been presented for a degree in this or other universities, all sources of materials used for this thesis work have been fully acknowledged.

Name: Addisalem Hailegnaw
Signature: ____________________

Place: Addis Ababa Institute of Technology, Addis Ababa University, Addis Ababa, Ethiopia
This thesis has been submitted for examination with my approval as a university advisor

Dr. Dereje Shiferaw
Advisor's name

____
Signature

Acknowledgement

I wish to express my sincere gratitude and indebtedness to my advisor Dr. Dereje Shiferaw for his guidance and assistance during the preparation of this Thesis.

I am thankful to my family for their encouragement and support throughout the study. Also, I would like to thank my colleagues and my friends for their friendship and help.

Abstract

Guided missiles with respect to their capability to engage high speed, highly agile targets and capability to achieve precision end-game trajectory requires extremely accurate performance of all component systems. In order to develop systems that meet the required accuracies, integrated guidance and control (IGC) systems are currently being studied. These IGC architectures infuse the guidance and control systems into a single framework thereby promoting natural synergy among the missile subsystems. Compared with designing the guidance subsystem and control subsystem of missile separately, integrated guidance and control has many superiorities, such as improving performance, reducing implementation cost and maximizing the adjustability of missile. Integrated guidance and control uses the target states relative to the missile to directly generate fin deflections that will result in target interception. In addition to achieving target interception, the integrated guidance and control has the responsibility for ensuring the internal stability of the missile dynamics. In this thesis Integrated guidance and control for a missile is developed using sliding mode control, taking a more natural guidance parameters which are predicted impact point heading errors as sliding surfaces. Mathematical model of a generic missile is derived by using the equations of motion, and missile/target engagement kinematics equations of the collision course are developed. Theoretical analysis shows the effectiveness of Integrated sliding mode guidance and control and simulations are carried out to show two dimensional and three dimensional missile target engagement scenarios using proportional navigation guidance law, and missile airframe is simulated to show the response to fin deflection so as to integrate the guidance law and control law later.

Key words: *Guided Missile, Mathematical Model of Missile, Integrated Guidance and control, Sliding Mode Control, Sliding Surface, Predicted impact point, Heading error, Proportional navigation*

Contents

List of Figures

List of Tables

Chapter 1

Introduction

A Missile is any object that can be projected or thrown at a target.This definition includes stones and arrows as well as gun projectiles, bombs, torpedoes, and rockets. In current warfare usage, the word Missile is gradually becoming synonymous with Guided Missile. A Guided Missile is an unmanned vehicle that travels above the earth's surface; it carries an explosive warhead or other useful payload;and it contains within itself some means for controlling its own trajectory or flight path[4] A historical review of early missile development can be found in[5].
In general missile systems can be categorized into two classes: strategic or tactical. Strategic missiles are designed to travel long distances towards known, stationary targets. Tactical missiles track or intercept shorter range, maneuvering and non-maneuvering targets where its guidance and control technologies turn out to be more critical[6].
Missiles are classified by the physical areas of launching and the physical areas containing the target. The four general categories of guided missiles are[7]:

1. Surface-to-Surface Missile (SSM)
2. Surface-to-Air Missile (SAM)
3. Air-to-Surface Missile (ASM) and
4. Air-to-Air Missile (AAM)

1.1 Missile Structure

Missiles are made of various sub-assemblies such as airframe, flight control system, guidance and targeting system, engine, warhead, fuze, propulsion, data link and radome[8]. The missile components are shown in figure 1.1.

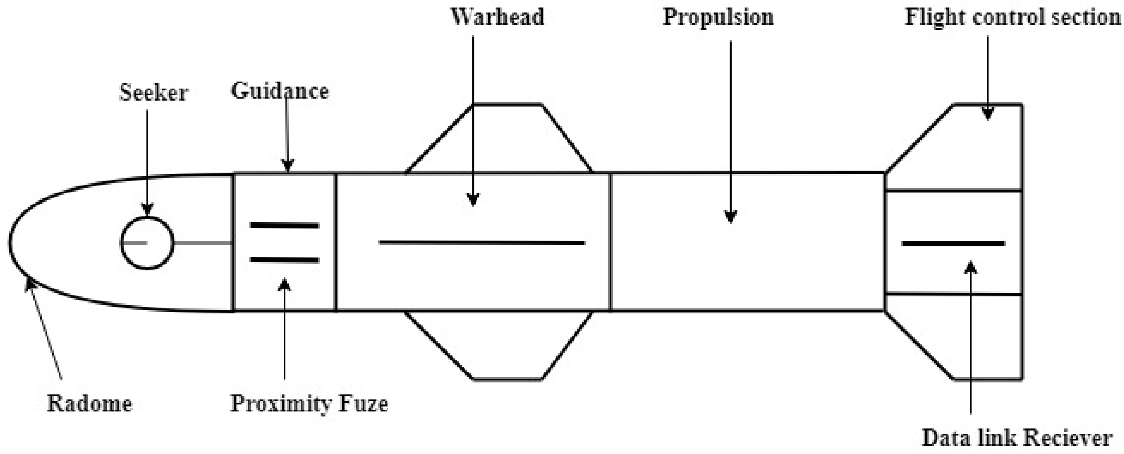

Figure 1.1: Missile Structure

Airframe: The airframes which carry the missile components are classified based on their source of lift and controls, i.e., the location of control surfaces such as wings, tails, and canards.
Flight Control: The flight control system uses pitch, yaw, and roll autopilots which control the airframes motions to provide stable, controlled, and responsive missile. These autopilots are automatic feedback control systems. The pitch and yaw autopilots are also known as lateral autopilots.
Guidance: The guidance system provides steering commands to lateral autopilots that would allow the missile to reach a successful intercept of the target. The guidance system performs four major functions in order to make a decision namely seeker stabilization, target acquisition, tracking and steering signal generation.
The Fuze: Every warhead must have a fuze. The fuze is that component (device) of the armament which recognizes the optimum time for detonation and initiates the detonation of the warhead at that particular time.
Warhead: A warhead is a device made of incendiary toxic materials and explosives used to deliver destructive force on to the enemy targets which may include military bases, missile launching sites, warships, tanks, etc. These are used in military conflicts and are delivered by a rocket, torpedo, or a missile.

1.2 Standard Terminologies in Missile Guidance

Lateral Acceleration: This is the acceleration that the missile needs to apply in order to achieve a desired turn rate. It is called lateral acceleration since it is usually applied in a direction close to the normal to the missile longitudinal axis or the missile velocity vector.
Line-of-Sight (LOS) Rate: During a missile-target engagement the imaginary line joining the missile and the target at any given instant in time is called the instantaneous line-of-sight or the LOS. This line changes in length and orientation as the engagement proceeds. The change in its angular orientation is given by its angular velocity or rate of turn and is usually expressed in units of $radians/sec$.

This is called the LOS rate.
Miss Distance: This is the distance of closest approach of the missile to the target. When the missile directly hits the target, the miss distance is zero. But when the missile passes close to the target the miss distance is non-zero. In this case the proximity fuze detonates the warhead and the engagement comes to an end. the primary objective of a guidance system is to minimize the miss-distance and the miss-distance is a non-negative quantity.
Closing Velocity: This is the velocity with which the missile closes on to the target. Obviously this is given by the rate at which the length of the LOS or the LOS separation shrinks. Hence, it is the negative of the rate of change of the LOS separation or range rate.
Time-to-Go : The time-to-go is an important trajectory parameter which is used for the implementation of many advanced guidance laws. Suppose we record the trajectory data of a missile-target engagement and find that the engagement ends with an interception at time t_f (final time). Note that interception is assumed to have taken place when either the missile directly hits the target or at the time of closest approach. Now, at any given instant in time t during the engagement the time-to-go is defined as the time remaining till interception and is given by $(t_f - t)$ and it is denoted as t_{go}. This value is the actual time-to-go which is known only after the engagement is over. But, to implement the guidance law, we need to estimate the t_{go} during the engagement.
Heading Error: The heading error is the difference in angle between the actual missile velocity vector and the angle required by the missile velocity vector to satisfy the collision geometry conditions. This parameter is an important performance measure for missiles that follow the mixed guidance scheme and have to transit from a command phase to a homing phase.

1.3 Missile Guidance

The term "Guidance" implies that the missile responds to steering commands in order to improve it's accuracy in delivering the warhead. Over the last 30 years, there have been many studies in the area of missile guidance. The result has been a great deal of progress, and several approaches to the problem have emerged. The basic problem is to intercept a target with great accuracy in an environment that is uncertain and noisy[1]. One of the earliest forms of missile guidance is that of command to line-of sight guidance. This involves establishing a line of sight between the tracking sensor and the target, as shown in figure 1.2 There are four positions to be identified in order that the geometry be defined. These are the tracking radar, the missile position, the target position, and the impact point. The missile is commanded onto or along the line of sight by use of a command link. Hence, the missile is fairly simple and only needs a communication link back to the guidance computer, which is usually located with the tracking sensor.

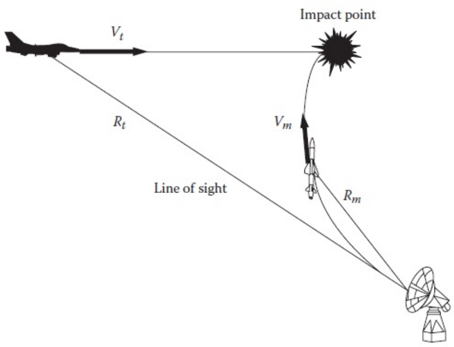

Figure 1.2: Command to line-of-sight guidance[1].

The guidance computer and the tracking sensor can be located on a stationary platform, such as a ground station for area defense, or on a mobile platform, such as an aircraft or helicopter. This form of guidance is usually short range as a line of sight has to be established between the tracking sensor and the target and maintained over the whole of the engagement. It also requires an accurate tracking sensor for both the target and the missile and a means to discriminate between the two.

The other form of guidance is homing guidance, which has become the predominant mode of guidance in the recent past. The geometry of the guidance of homing missiles is shown in figure 1.3

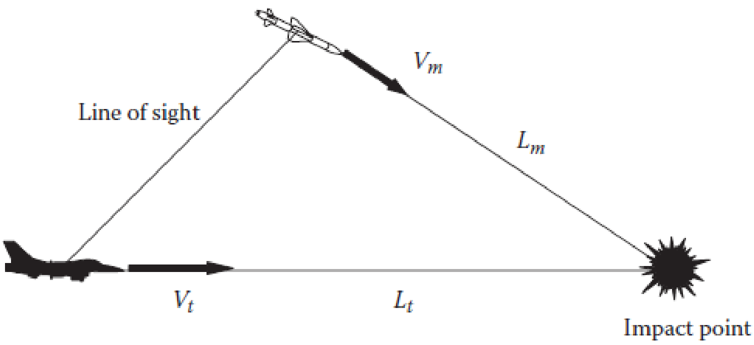

Figure 1.3: Homing Geometry

There are three reference points defining the engagement geometry:

1. the missile plus homing head position.
2. the target position, and
3. the impact point.

If the tracking sensor is placed in the nose of the missile, the sensor will get closer to the target as the engagement progresses. This makes the tracking of the target easier, but the main disadvantage is that the sensor must fit into the diameter of the missile and consume power that is stored on board. Hence, the range and

accuracy of the tracking sensor are much less than those of the line-of-sight guidance. The guidance computer also has to be carried on board; hence, its size and power will also be reduced in comparison. All of these facts make the homing missile more complex and costly than the line-of-sight missile. The main advantage of the homing missile is the fact that when launched, it does not require a separate tracking sensor, which could become vulnerable to counter-attack. It also means that several homing missiles can be launched at the same time. There has been a lot of interest in the development of homing guidance techniques in the literature, mostly on two themes: that of proportional navigation and the use of more modern control techniques such as optimal control. Variants on the proportional navigation algorithm that improve the performance against maneuvering targets have been proposed.
All of these rely on accurate measurements that can position the missile and the target, as well as estimate the target motion in terms of a velocity and acceleration vector. The main way of doing this is by means of the tracking sensor, which measures properties of the sight line between the missile and the target. Most guidance algorithms rely on the line-of-sight rotation rate and target relative range, with extra information coming from the range rate if available.Modern trends are to also obtain information from third-party sensors with a networked capable system, but this is usually for the midcourse guidance phase where the tracking sensor is not active.

1.4 Homing Missile Target Sensors

In the homing guidance system, the missile has a homing device on-board which can detect the target and gives the necessary path directions for intercept to the missile. The purpose of the seeker is to detect, acquire and track a target by sensing radiation or reflected energy from the target. The seeker carried on board a homing missile is categorized as one of the following three general types[2]:

1. Passive
2. Semi-active
3. Active

Active detection is when the missile illuminates the target, i.e., with a radar, and receives the reflected signals. Semi-active detection is when the target is illuminated by a source other than the missile and the missile receives the reflected signals. Passive detection is used when the target is the source of energy, and the missile detects signals that propagate from the target. Figure 1.4 conceptually illustrates the three types of homing missile seekers. Common examples of passive systems are infrared (IR) and radio-frequency (RF) seekers. IR seekers detect and track the natural heat signature emanating from a target, whereas passive RF seekers detect stray, or otherwise reflected, RF energy from the target. A passive seeker does not illuminate the target but, instead, receives energy that emanates from it. Because they do not emit energy, passive seekers make it impossible for the target to determine whether it is being tracked. Semi-active guidance systems illuminate, or designate, the target by directing a beam of light, laser, IR, or RF energy at it. The illuminating beam is transmitted from the launch platform or from an adjacent location. Hence, the

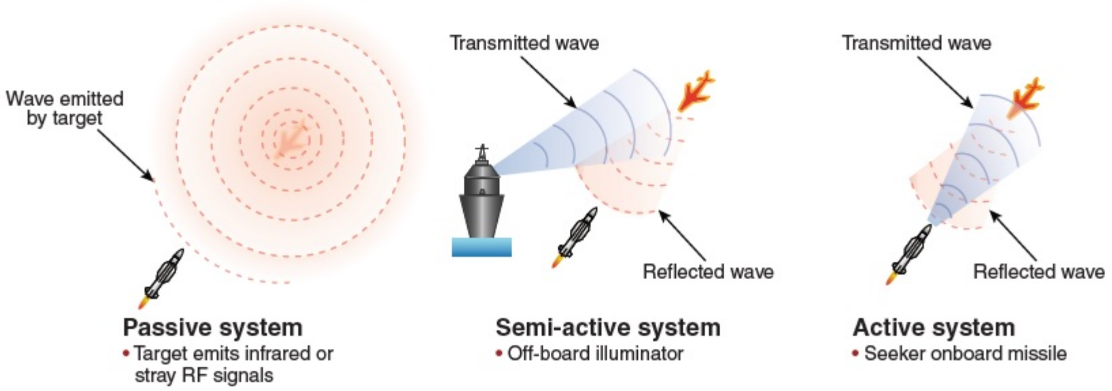

Figure 1.4: Types of missile seeker systems[2]

illuminating source is largely responsible for target selection in a semi-active system. The passive seeker in the missile then tracks the target using the energy reflected from it. In active seeker guidance systems, an illuminator (transmitter) is added to the missile. Hence, an active guidance system can self-illuminate the target. The addition of an illuminator is costly and adds weight to the missile. However, the missile then is self-sufficient and autonomous after it has locked onto the target.
Passive seekers measure the angular direction of the target relative to the missile, but they do not readily provide range to target or closing velocity (range-rate) information,which is a potential disadvantage in that some guidance techniques require target range and/or range-rate information in addition to azimuth and elevation angles. In these cases, other means of obtaining this information must be employed.

1.5 Conventional and Integrated Guidance and Control

Traditional approach to the design of missile control and guidance systems has been to neglect the interactions between the guidance and autopilot system and to treat individual missile subsystems separately. The missile dynamics is split into translational and rotational components. The translational dynamics is used to synthesize the guidance law, while the rotational dynamics is employed to design an autopilot to stabilize the missile and to track guidance commands. Designs are generated for each subsystem and these designs are then assembled together. If the overall system performance is unsatisfactory, individual subsystems are re-designed to improve the system performance. Due to its iterative nature, this latter part of the design process can be highly time-consuming[9].
Figure 1.5 illustrates traditional guidance-control systems. In the conventional approach, the guidance law does not employ the missile body rates or the sensed acceleration components to generate the commands to the autopilot. As a result, in engagement scenarios requiring agile maneuvers, the guidance commands can often exceed autopilot performance limits. If the autopilot employs integral feedback loops for improved command tracking response, these guidance commands can drive the flight control system unstable. Additionally, since the autopilot does not use target relative missile position and velocity components for feedback, it cannot adjust its

response to accommodate for agile target maneuvers. Consequently, the traditional design approach requires the autopilot to have a small time constant when compared with the guidance system to assure the stability and performance of the overall flight control system.

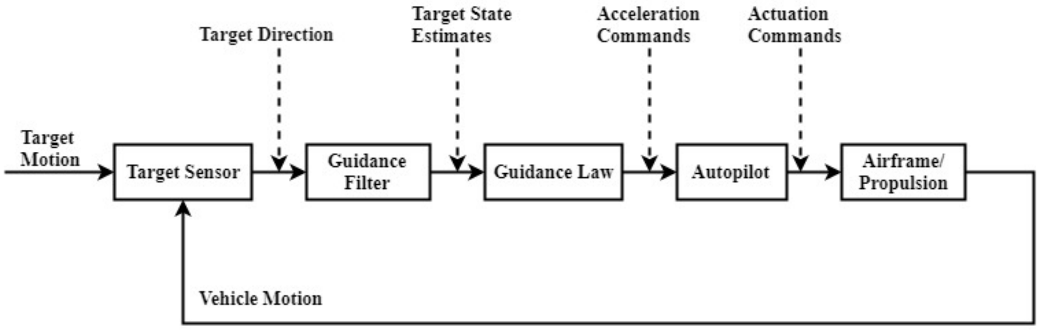

Figure 1.5: Conventional Missile Guidance and Control System

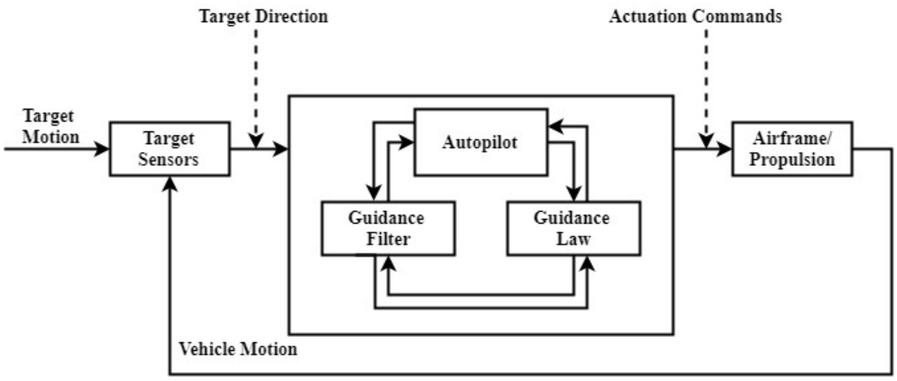

Figure 1.6: Integrated Guidance and Control System

Figure 1.6 illustrates Integrated guidance-control systems. In the integrated approach, the guidance and autopilot functions use all the available measurements. As a result, the system is less likely to encounter saturation and stability problems. Moreover, the iterative design steps required to ensure the compatibility between the guidance and autopilot systems are eliminated from the process.

Exploiting the synergistic coupling that exists between the guidance (i.e., the information and prediction aspect of the problem) and flight control functions helps to achieve optimal interceptor performance. In contrast to the decoupled approach, a tightly integrated G&C (IGC) paradigm facilitates G&C synergism in addition to offering a structured approach to performance optimization[10].

Many missile subsystems have interactions that can be exploited to optimize performance. For instance, at the G&C component level, an inverse relationship exists between information and prediction quality (i.e.,guidance system accuracy) versus the necessary bandwidth of the flight control system to render a kill. An IGC system can explicitly accommodate this relationship.

1.6 Statement of the problem

The problem is to find a way by which the missile can hit the target. Modern guided missiles must engage and negate a variety of threats, including tactical ballistic missiles and high-performance cruise missiles. The need to engage such diverse and ever-evolving threats poses a significant challenge to missile guidance and control design. The classical missile guidance and control approach involves treating the guidance and control systems as two separate processes. This Guidance and control approach involves time-consuming iterative loops between the guidance and control subsystems. Separate designs and weak functional interactions between the algorithms make interceptor performance optimization difficult.
The Guidance and Control system must functionally integrate and orchestrate the various missile subsystems to ensure that all requirements are met and that lethality is consistently maximized across the range of threats of interest. An alternative that can yield better overall performance while avoiding the iterative loops is an integrated guidance and control approach.
The Missile system is a highly nonlinear, highly varying dynamical system which is subject to external disturbances and heavy model uncertainties with complex control capabilities. Due to the rapid change in velocity and dynamic pressure, plant parameters change rapidly. Besides these changes, the desired angle of attack region is also too wide. Consequently, for an application of practical Guidance, a guidance law should be as robust as possible towards these changes. To design the Integrated Guidance and Control for a missile, the robust control method is needed because of the above problems.Thus, to solve the Integrated guidance and control problem Sliding Mode control can be used. Sliding mode control strategy which allows controlling non-linear processes subject to external disturbances and heavy model uncertainties can be used since it is robust to parameter perturbations and external disturbances. It also maintains stability and performance in the presence of modeling errors. The present thesis addresses the design and evaluation of a missile using sliding mode control for Integrated Guidance and control strategy.

1.7 Objectives

1.7.1 General Objective

The general objective of this thesis is to design Sliding mode integrated Guidance and control for a Missile; which insures that the lethality is consistently maximized.

1.7.2 Specific Objectives

- To develop Equations of motion and two/three dimensional Missile-target engagement kinematics.
- To analyze the synergistic coupling between guidance and control.
- To develop control laws using sliding mode control based on the selected sliding surfaces.
- To analyze the performance of sliding mode Integrated guidance and control and to simulate sample missile target engagement scenarios.

1.8 Organization of the thesis

This thesis consists of a Missile target Engagement Scenario, guidance design, and also the test simulation is conducted for different initial conditions and with different target maneuvers. As a summary;

- Chapter 1 States basic definitions about Missiles and Missile Guidance, includes methodology.
- Chapter 2 Is literature review.
- Chapter 3 starts with coordinate frames, it continues with missile equations of motion and 2D/3D missile-target engagement scenarios different engagement kinematics for different guidance law development mechanisms. pitch-plane and yaw-plane are defined and different components corresponding to each plane are obtained.
- Chapter 4 describes sliding mode control(SMC) theory, Terminal Sliding mode Control(TSM), and Integrated sliding mode guidance and control design for pitch and yaw planes.
- Chapter 5 includes the simulation studies for how the airframe responds to fin deflections and proportional navigation guidance law is applied with different interception scenarios from easy to hard difficulty levels to show that it can be used for the simulation development of sliding mode integrated guidance and control.

Chapter 2

Literature Review

When the application of Integrated Guidance and Control(IGC) scheme to homing missiles was first addressed in 1984, an optimal controller was designed to combine the conventionally separated guidance law design and autopilot design into one framework by minimizing a quadratic cost function subject to intercept dynamics. The Integrated Guidance and Control design resulted in better RMS miss, the terminal angle of attack, the pitch rate, and the control surface flapping rate in the presence of unmodeled errors[1]. Optimal control is one of the most widely used theories in modern control, and has been widely used in the integrated design of guidance and control[11]. In the paper "Non-linear Integrated Guidance-Control Laws For Homing Missiles." by Ernest J. Ohlmeyer and P. K. Menon [9], integrated guidance-control techniques for homing missiles are discussed. They employed the feedback linearization method in conjunction with the linear quadratic regulator technique to design a set of nonlinear Integrated Guidance Control laws for homing missiles. Three different formulations for the integrated design of homing missile guidance and control systems are discussed.The first method employs the yaw and pitch components of the zero effort miss (ZEM) vector as the primary state variables. The second formulation employs the pitch-yaw components of the missile relative target position as the primary state variables. The third formulation is an integrated guidance-control analog of the classical proportional navigation algorithm.
Sliding mode variable structure control was superior to its invariance for the interference in the sliding mode, and the algorithm was relatively simple, so the sliding mode variable structure control theory was widely used in the missile guidance and control system design[12]. Padhi et al.[13] designed the missile integrated guidance and control system based on the sliding mode variable structure control theory. The simulation experiments showed that, compared with the traditional "spectral separation" design method, this method had superiority on control and guidance accuracy.
Shkolnikov et al. [14] used first-order Sliding Mode Control to develop an Integrated Guidance and Control system for a homing interceptor. They investigated the line-of-sight (LOS) rate and the transversal relative velocity component as possible sliding surfaces and developed guidance and control laws based on methods previously developed by other researchers. An inner-loop/outer-loop approach was used, with the outer loop creating a commanded pitch rate that was tracked in the inner loop via the pitch fin deflection.Shkolnikov et al. later modified their approach using second-order sliding mode rather than the first-order one as was used in the previous study.

In Shima et al.s paper [15], the zero-effort miss(ZEM) distance is used as the sliding surface. Unlike the previous sliding mode approaches to IGC, the authors formulated the guidance and control systems together in one loop and established a direct relationship between the control input and guidance objective. Performance of the integrated approach was compared to that of two different inner-loop/outer-loop designs, and it was shown that the integrated controller led to superior results.
There have also been several approaches to solving the Integrated Guidance and Control problem by using the sliding mode control (SMC) techniques. Ali Amer Ahmed Alrawi et al. in [16] adopted The modified sliding mode controller (MSMC) algorithm to enable the missile to reach the desired target within a short period of time. In this paper, Guidance and Control algorithms coordinate the various missile subsystems to ensure that all applicable requirements are met and to consistently maximize the destruction caused by missiles.A missile guidance law takes target data and integrates them with knowledge about the missile state to generate acceleration commands to place the missile within the line-of-sight (LOS) of the target.This paper addresses an application of the sliding mode control to design a robust missile command guidance law. To confirm the effectiveness of the proposed MGCSMC algorithm, the application of G&C to the high-altitude flight angle of a SAM(surface to air missile) was simulated. In this simulation, the missile successfully reached the destruction area of the target for all cases of the manoeuvering target. The proposed MGCSMC method had high accuracy of destruction although it took some time for the method to achieve 100% accuracy for the high-altitude target.
The focus of the present thesis is on the development of integrated guidance and control systems for a homing missile using Sliding mode technique. In this case Missile-Target engagement kinematics and missile dynamics are integrated into one state space, and the intercept problem is transformed into the output regulation problem, which is addressed using terminal sliding mode based control for the missile aerodynamic surface actuator. All Sliding Mode Control guidance algorithms include smoothing procedures that yields partial loss of robustness to disturbances and uncertainties but, the guidance law must be smooth, in this thesis this problem is addressed in the frame of Higher Order Sliding Mode(Terminal Sliding Mode) Technique

Chapter 3

Mathematical Modeling

The goal of any missile guidance and control scheme is to steer the missile so as to impact the target in a finite period of time. With the Integrated Guidance and Control system developed in the missile body frame, the dynamics are derived so that the fin deflections control the motions of the missile. The fins primarily adjust the orientation of the missile, and then the resulting incident flow produces forces that provide translational motion for the missile. In the body-based Integrated Guidance and Control formulation, this dominant effect of fin deflection results in the rotational errors to be regulated more effectively than velocity errors. This phenomenon results in the missile actually sliding around the target instead of correctly steering toward the target. It became evident that body based Integrated Guidance and Control formulation was unable to accurately capture the physics behind missile motion[1],[17]. If the target is traveling with a constant direction and the missile is traveling in the desired direction for impact, then the Predicted Impact Point will be fixed in space. Given these circumstances, the goal of the missile guidance and control scheme can be construed as steering the missile velocity toward a fixed point in space, the Predicted Impact Point,which will minimize the final miss distance. The missile is controlled via fin deflections, which creates a torque on the missile. When the missile rotates, the incoming air impacts the missile with an angle of attack and side-slip angle which in turn creates a restoring moment and a normal force which turns the missile.

Mathematical modeling of the missile incorporates different definitions such as coordinate systems, aerodynamic model, equations of motion, control surface deflection and control actuation system. Equations of motion that are required to define a missile motion which contains kinematic and dynamical equations. Both of the kinematic and dynamic equations can be divided into two parts as translational and rotational equations of motion. Euler angles are used to define the conversion between coordinate systems and also makes connection between these rotational kinematics and rotational dynamics. Dynamical equations are basically defined by using Newtons second law of motion that relates the translational accelerations to forcesand the rotational accelerations to moments. In this chapter, coordinate systems are presented to define the relative motion of the missile. Nonlinear mathematical model is derived by using equations of motion that includes aerodynamic model.

3.1 Coordinate Frames

3.1.1 Inertial Frame

The inertial frame is fixed with its origin at the center of the earth and has no acceleration and rotation relative to stars as seen in Figure 3.1

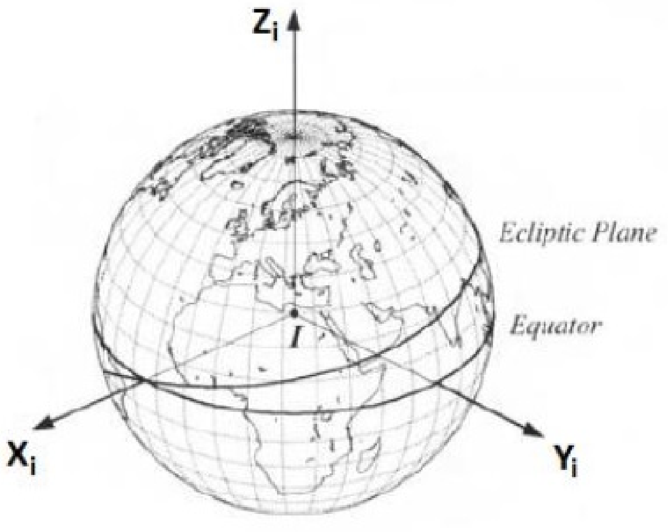

Figure 3.1: Inertial reference coordinate system [3]

X_i direction is defined as the vector from the center of the Earth pointed to the Sun and passes through the intersection of the ecliptic plane and the equator in spring. Inertial sensors that are used in inertial navigation systems measures acceleration and rates with respect to inertial coordinate system.

Origin : Center of the Earth, Xi axis: Direction of vernal equinox,
Y_i axis: Orthogonal to the X_i and Z_i direction according to the right hand rule,
Z_i axis: Directed to the North pole.

3.1.2 Local Cartesian Frame

To represent the relative distances between missile and target and also the trajectory that missile follows, there is a need to define a coordinate system. In addition, guidance algorithms also needs the relative Cartesian locations between missile and target. Local Cartesian coordinate system is defined to supply these needs.

Origin : Projection of where motion of missile starts on zero altitude,
X_c : Directed to ellipsoid north,
Y_c : Directed to ellipsoid east,
Z_c : Directed to ellipsoid down.

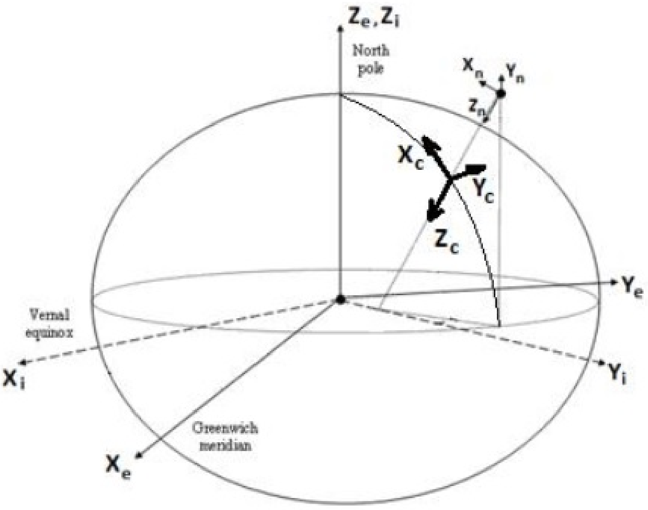

Figure 3.2: Local Cartesian coordinate system definition

3.1.3 Body Frame

The origin of the body coordinate system is linked to the missile body and the center of mass. Its axes are X_b, Y_b, Z_b. The $x-$axis, called the roll axis, points towards the nose of missile; the $y-$axis, called the pitch axis is directed to right when the missile viewed from rear and orthogonal to X_b. The $z-$axis is directed according to the right hand rule.

Origin : Center of gravity of missile,
X_b : Directed from center of the coordinate system the nose of missile,
Y_b : When viewed from rear directed to right. Orthogonal to X_b,
Z_b : Orthogonal to the X_b and Y_b direction according to the right hand rule.

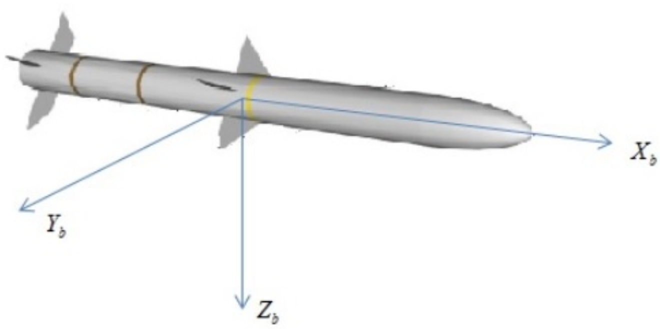

Figure 3.3: Body coordinate system at the center of gravity of missile

A vector defined in one coordinate system can be redefined in another coordinates system. This is achieved by axis transformations. Any set of axes definition of a vector can be obtained from any other set by a sequence of three rotations. For each rotation, a transformation matrix is applied to the vectorial quantities. The final transformation matrix is simply the product of the three matrices, multiplied in the order of the rotations. Common law of the aeronautics states that firstly rotate the system by ψ(yaw angle) about Z axis, then by θ (pitch angle) about new Y axis, and by ϕ (roll angle) about the latest X axis which are called Euler Angles. The transformation matrices are defined with order of rotation about $Z, Y and X$ axis.

The first rotation about Z axis (ψ angle):

$$\begin{bmatrix} X_2 \\ Y_2 \\ Z_2 \end{bmatrix} = C_\psi \begin{bmatrix} X_1 \\ Y_1 \\ Z_1 \end{bmatrix} = \begin{bmatrix} cos(\psi) & sin(\psi) & 0 \\ -sin(\psi) & cos(\psi) & 0 \\ 0 & 0 & 1 \end{bmatrix} \begin{bmatrix} X_1 \\ Y_1 \\ Z_1 \end{bmatrix}$$

The second rotation about Y axis (θ angle):

$$\begin{bmatrix} X_2 \\ Y_2 \\ Z_2 \end{bmatrix} = C_\theta \begin{bmatrix} X_1 \\ Y_1 \\ Z_1 \end{bmatrix} = \begin{bmatrix} cos(\theta) & 0 & -sin(\theta) \\ 0 & 1 & 0 \\ sin(\theta) & 0 & cos(\theta) \end{bmatrix} \begin{bmatrix} X_1 \\ Y_1 \\ Z_1 \end{bmatrix}$$

And the third rotation about X axis (ϕ angle) is stated as follows.

$$\begin{bmatrix} X_2 \\ Y_2 \\ Z_2 \end{bmatrix} = C_\phi \begin{bmatrix} X_1 \\ Y_1 \\ Z_1 \end{bmatrix} = \begin{bmatrix} 1 & 0 & 0 \\ 0 & cos(\phi) & sin(\phi) \\ 0 & -sin(\phi) & cos(\phi) \end{bmatrix} \begin{bmatrix} X_1 \\ Y_1 \\ Z_1 \end{bmatrix}$$

This sequential rotations defines a transformation matrix called Direction Cosine Matrix that will define a transformation of a motion from Earth coordinate system to body coordinate system as follows.

$$\begin{bmatrix} X_b \\ Y_b \\ Z_b \end{bmatrix} = C_\phi C_\theta C_\psi \begin{bmatrix} X_e \\ Y_e \\ Z_e \end{bmatrix}$$

$$= \begin{bmatrix} cos(\psi) & sin(\psi) & 0 \\ -sin(\psi) & cos(\psi) & 0 \\ 0 & 0 & 1 \end{bmatrix} \begin{bmatrix} cos(\theta) & 0 & -sin(\theta) \\ 0 & 1 & 0 \\ sin(\theta) & 0 & cos(\theta) \end{bmatrix} \begin{bmatrix} 1 & 0 & 0 \\ 0 & cos(\phi) & sin(\phi) \\ 0 & -sin(\phi) & cos(\phi) \end{bmatrix} \begin{bmatrix} X_e \\ Y_e \\ Z_e \end{bmatrix}$$

$$\begin{bmatrix} X_b \\ Y_b \\ Z_b \end{bmatrix} = C^{(b,e)} \begin{bmatrix} X_e \\ Y_e \\ Z_e \end{bmatrix}$$

This representation stands for the transformation from the Earth axis to the body axis system.

$\left[C^{(b,e)}\right]^{-1} = \left[C^{(b,e)}\right]^{T} = C^{(e,b)} \implies \begin{bmatrix} X_e \\ Y_e \\ Z_e \end{bmatrix} = C^{(e,b)} \begin{bmatrix} X_b \\ Y_b \\ Z_b \end{bmatrix}$ represents the transformation from body axis to Earth axis.

3.2 Aerodynamic model

3.2.1 Flight parameters

Angle of Attack:

The angle between the projection of velocity vector of missile on $x_b - z_b$ plane and x_b axis of missile in longitudinal plane. It is positive when the missile velocity component along $z-$axis is positive.

Angle of Sideslip :

The angle between the projection of velocity vector of missile on $x_b - y_b$plane and X_b axis of missile in lateral plane. It is positive when the missile velocity component along $y-$axis is positive.

Mach Number:

In fluid mechanics, it represents the ratio of speed of an object moving through a fluid and the local speed of sound. C represents the speed of the sound, then Mach number can be expressed as

$$M = \frac{V}{C}$$

C can be stated as $C = \gamma RT$ where γ is the specific heat ratio of the air which is taken to be equal to 1.4, and R is the universal air gas constant which is equal to $287J/kgK$. T is the ambient temperature which changes with altitude, and can be expressed as

$$T = \begin{cases} T_o(1 - 0.00002256h), & \text{for } h <= 1000m. \\ 0.7744T_o, & \text{for } h > 1000m. \end{cases}$$

Dynamic Pressure:

It is defined as

$$Q = \frac{1}{2}\rho V^2$$

The term ρ is the air density.

3.2.2 Aerodynamic Forces and Moments

Aerodynamic forces and moments can be represented with their coefficients. If reference area is A, reference length is d, dynamic pressure is Q and C_X, C_Y and C_Z are aerodynamic coefficients for forces respectively, then the aerodynamics forces can be stated as follows

$$\begin{bmatrix} F_{ax} \\ F_{ay} \\ F_{az} \end{bmatrix} = QA \begin{bmatrix} C_X \\ C_Y \\ C_Z \end{bmatrix}$$

For C_l, C_m, and C_n are moment coefficients, aerodynamic moments can be stated as

$$\begin{bmatrix} L \\ M \\ N \end{bmatrix} = QAd \begin{bmatrix} C_l \\ C_m \\ C_n \end{bmatrix}$$

where

C_X : Axial force coefficient,

C_Y : Side force coefficient,

C_Z : Normal force coefficient,

C_l : Rolling moment coefficient,

C_m : Pitching moment coefficient,

C_n : Yawing moment coefficient

Aerodynamic coefficients can be stated to be a function of several flight variables as $C_i = C_i(M, \alpha, \beta, \delta_a, \delta_e, \delta_r, p, q, r, \dot{\alpha}, \dot{\beta})$ In real world, these coefficients are functions of much more flight parameters and higher order terms. Force and moment coefficients can be found from look up tables that are created from Mach number, angle of attack, angle of sideslip, elevator fin deflection (δ_e), aileron fin deflection (δ_a), and rudder fin deflection (δ_r).

3.3 Equations of Motion

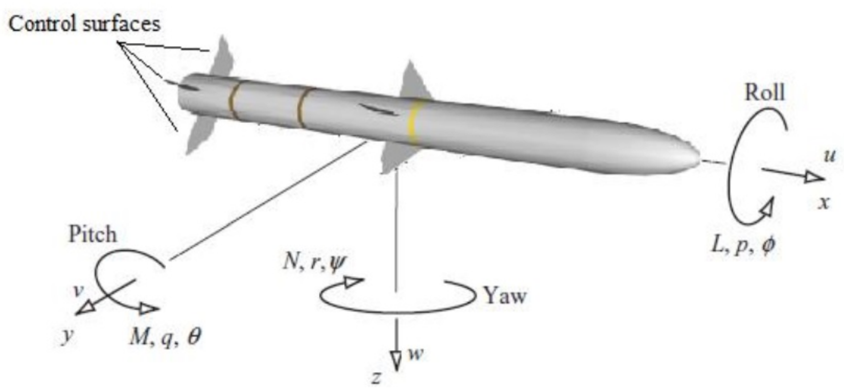

Figure 3.4: Translational and rotational definitions

The parameters related to the missile are defined in Table 3.1. Two assumptions are made before starting the derivation[18]:

- mass of the missile remains constant
- missile is a rigid body.

Table 3.1: Related parameters of missile

	X	V	Z
Angle	$\phi(roll)$	$\theta(pitch)$	$\psi(yaw)$
Velocity	U	V	W
Position	X_b	Y_b	Z_b
Angular rate	p	q	r
Force	F_x	F_y	F_z
Moment	L	M	N
Inertia	I_{xx}	I_{yy}	I_{zz}
Product of inertia	I_{yz}	I_{xz}	I_{xy}

The forces and moments acting on a missile are given as F_X, F_Y, F_Z and M_x, M_y, M_z. These forces and moments are total of some distinct forces and moments. Aerodynamic forces, thrust forces and the gravitational effects have to be taken into consideration while talking about these forces and moments. In fact, these forces and moments can be written as

$$\begin{bmatrix} F_X \\ F_Y \\ F_Z \end{bmatrix} = \begin{bmatrix} F_{ax} + mg_x + T_x \\ F_{ay} + mg_y + T_y \\ F_{az} + mg_z + T_z \end{bmatrix}$$

$$\begin{bmatrix} M_X \\ M_Y \\ M_Z \end{bmatrix} = \begin{bmatrix} L + L_T \\ M + M_T \\ N + N_T \end{bmatrix}$$

In the above equations, $F_{ax}, F_{ay}, F_{az}, F_{ay}, L, M$ and N are the forces and moments which only occurs due to aerodynamics effects on the missile flight. g_x, g_y, and g_z are the body frame components of the gravitational acceleration which is assumed to be oriented directly towards the Earth center. $T_x, T_y, T_z, L_T, M_T, N_T$, are thrust force and thrust moment components.

3.3.1 Kinematic Equations of Motion

Translational Kinematics

Velocity expressed in the body coordinate system can be transformed to the Earth coordinate system by using the transpose of Direction Cosine Matrix that is calculated before.

$$\begin{bmatrix} V_X \\ V_Y \\ V_Z \end{bmatrix} = C^{(e,b)} \begin{bmatrix} u \\ v \\ w \end{bmatrix}$$

and if the calculation is extended, the following equations are obtained.

$$\begin{aligned} V_X = (cos(\theta)cos(\psi))u + (sin(\phi)sin(\theta)cos(\psi)cos(\phi)sin(\psi))v \\ +(cos(\phi)sin(\theta)cos(\psi) + sin(\phi)sin(\psi))w \end{aligned} \tag{3.1}$$

$$\begin{aligned} V_Y = (cos(\theta)sin(\psi))u + (sin(\phi)sin(\theta)sin(\psi)cos(\phi)cos(\psi))v \\ +(cos(\phi)sin(\theta)sin(\psi) + sin(\phi)cos(\psi))w \end{aligned} \tag{3.2}$$

$$V_Z = (sin(\theta))u + (sin(\phi)cos(\theta))v + (cos(\phi)cos(\theta))w \tag{3.3}$$

where V_X, V_Y and V_Z are the velocity components of the body with respect to the Earth fixed frame stated in Earth fixed frame and u, v, w are the velocities with respect to Earth fixed frame stated in body frame.

Rotational Kinematics

The rotational kinematic equations relates the time rate of change of the Euler angles(orientation of missile with respect to the reference coordinate frame) to the angular rates of missile body. Using the identity feature

$$\left[C^{(e,b)}\right]^T C^{(e,b)} = 1 \tag{3.4}$$

it is known that derivative of a constant is zero.

$$\begin{aligned} \frac{d}{dx}\left(\left[C^{(e,b)}\right]^T C^{(e,b)}\right) &= \frac{d}{dx}(I) \\ \left[C^{(e,b)}\right]^T C^{(e,b)} &= \left[-C^{(e,b)}\right]^T C^{(e,b)} \\ \left[C^{(e,b)}\right]^T C^{(e,b)} &= -\left(\left[C^{(e,b)}\right]^T C^{(e,b)}\right) \end{aligned} \tag{3.5}$$

The above equation indicates that $\left[C^{(e,b)}\right]^T C^{(e,b)}$ is a skew symmetric matrix and so there exists a skew symmetric $\vec{w}$ generated from a column $\vec{w}$ such that $\vec{w} = \left[C^{(e,b)}\right]^T C^{(e,b)}\vec{w}_{ang}$ is composed of the components of the angular velocity of the body frame with respect to the Earth frame stated in body frame. More explicitly,

$$\vec{w}_{ang} = \begin{bmatrix} p \\ q \\ r \end{bmatrix}$$

thus the corresponding skew symmetric matrix is

$$\vec{w} = \begin{bmatrix} 0 & -r & q \\ r & 0 & -p \\ -q & p & 0 \end{bmatrix}$$

Solving $\left[C^{(e,b)}\right]^T C^{(e,b)} = \vec{w}$ for the Euler angle rates, the rotational kinematical equations are found as

$$\begin{aligned} \dot{\phi} &= p + (qsin(\phi) + rcos(\phi))tan(\theta) \\ \dot{\theta} &= qcos(\phi)rsin(\phi) \\ \dot{\psi} &= \frac{qsin(\phi) + rcos(\phi)}{cos(\theta)} \end{aligned} \tag{3.6}$$

3.3.2 Dynamical Equations of Motion

Translational Dynamics

For derivation of translational dynamics, force equation of the Newtons Second Law is used as follows. If the Earth rotation with respect to the inertial frame is neglected, the Earth frame can be declared as the inertial frame then equations can be derived as if translational and angular velocities are defined in the Earth frame.

$$\begin{aligned} \vec{F} &= \frac{d}{dt}(m\vec{V})|_E = m\frac{d}{dt}(\vec{V})|_E \\ \vec{F} &= \vec{F}_{aero} + \vec{F}_{thrust} + \vec{F}_{gravity} \end{aligned} \tag{3.7}$$

where F is the sum of all externally applied forces acting on the missile including aerodynamic forces, thrust forces and gravity forces, m is the mass of missile, V is the velocity of center of mass with respect to the Earth frame. $|_E$ indicates that the differentiation of the related terms are done in the Earth frame. In the body frame, It can be written as

$$\vec{F} = m(\frac{d}{dt}\vec{V}|_B) + \vec{w}_{ang} \times \vec{V} \tag{3.8}$$

where $|_B$ indicates that the differentiation is done in the body frame. $\vec{F}$ vector is represented as

$$\vec{F} = \begin{bmatrix} F_X \\ F_Y \\ F_Z \end{bmatrix}$$

the linear velocity vector $\vec{V}$ is stated as

$$\vec{V} = \begin{bmatrix} u \\ v \\ w \end{bmatrix}$$

and the angular velocity vector is

$$\vec{w}_{ang} = \begin{bmatrix} p \\ q \\ r \end{bmatrix}$$

Then

$$\begin{bmatrix} F_x \\ F_Y \\ F_Z \end{bmatrix} = m \left\{ \begin{bmatrix} \dot{u} \\ \dot{v} \\ \dot{w} \end{bmatrix} + \begin{bmatrix} p \\ q \\ r \end{bmatrix} \times \begin{bmatrix} u \\ v \\ w \end{bmatrix} \right\}$$

After some manipulations

$$\begin{bmatrix} \dot{u} \\ \dot{v} \\ \dot{w} \end{bmatrix} = \begin{bmatrix} \frac{F_X}{m} \\ \frac{F_Y}{m} \\ \frac{F_Z}{m} \end{bmatrix} - \begin{bmatrix} qw - rv \\ ru - pw \\ pv - qu \end{bmatrix}$$

Finally translational equations are derived as

$$\begin{aligned} \dot{u} &= \frac{F_X}{m} - qw + rv \\ \dot{v} &= \frac{F_Y}{m} - ru + pw \\ \dot{w} &= \frac{F_Z}{m} - pv + qu \end{aligned} \tag{3.9}$$

Rotational Dynamics

For the derivation of rotational dynamic equations, following equality will be used

$$\vec{M} = \frac{d}{dt}(\vec{H})|_E \tag{3.10}$$

$\vec{M}$ represents the sum of all externally applied torques to missile. $\vec{H} = \hat{J}\vec{w}_{ang}$ is the angular momentum of the missile, $\hat{J}$ is the inertia dyadic. In the body coordinate system the Equation can be written as

$$\vec{M} = \hat{J}\left[\frac{d}{dt}(\vec{H})|_B\right] + \vec{w}_{ang} \times \hat{J}\vec{w}_{ang} \tag{3.11}$$

The inertia dyadic can be expressed in the body frame by the following matrix

$$\hat{J} = \begin{bmatrix} I_{xx} & -I_{xy} & -I_{xz} \\ -I_{xy} & I_{yy} & -I_{yz} \\ -I_{xz} & -I_{yz} & I_{zz} \end{bmatrix}$$

The body axis of the missile is taken to be coincident with the principle axis of inertia. Hence product of cross inertia terms I_{xy}, I_{xz} and I_{yz} vanish. Due to the symmetric structure of the missile used in this study, $I_{yy} = I_{zz}$ equality will be used. Thus the inertia matrix can be simplified for a symmetric missile as

$$\hat{J} = \begin{bmatrix} I_{xx} & 0 & 0 \\ 0 & I_{yy} & 0 \\ 0 & 0 & I_{zz} \end{bmatrix}$$

The column vector representation of total moment is

$$\vec{M} = \begin{bmatrix} M_X \\ M_Y \\ M_Z \end{bmatrix}$$

Thus,

$$\begin{bmatrix} M_X \\ M_Y \\ M_Z \end{bmatrix} = \begin{bmatrix} I_{xx} & 0 & 0 \\ 0 & I_{yy} & 0 \\ 0 & 0 & I_{zz} \end{bmatrix} \begin{bmatrix} \dot{p} \\ \dot{q} \\ \dot{r} \end{bmatrix} + \begin{bmatrix} p \\ q \\ r \end{bmatrix} \times \begin{bmatrix} I_{xx} & 0 & 0 \\ 0 & I_{yy} & 0 \\ 0 & 0 & I_{zz} \end{bmatrix} \begin{bmatrix} p \\ q \\ r \end{bmatrix}$$

After some calculations

$$\begin{bmatrix} M_X \\ M_Y \\ M_Z \end{bmatrix} = \begin{bmatrix} I_{xx}\dot{p} \\ I_{yy}\dot{q} \\ I_{zz}\dot{r} \end{bmatrix} + \begin{bmatrix} I_{zz}qr - I_{yy}qr \\ -I_{zz}pr + I_{xx}pr \\ I_{yy}pq - I_{xx}pq \end{bmatrix}$$

Finally rotational dynamic equations are obtained as

$$\begin{aligned} \dot{p} &= \frac{M_X - qr(I_{zz} - I_{yy})}{I_{xx}} \\ \dot{q} &= \frac{M_Y - rp(I_{xx} - I_{zz})}{I_{yy}} \\ \dot{r} &= \frac{M_Z - pq(I_{yy} - I_{xx})}{I_{zz}} \end{aligned} \tag{3.12}$$

3.3.3 Control Surface Deflection Angles

The missile considered in this study is a tail controlled missile and flies in X configuration as seen in Figure 3.5 . Direction of the arrows show the positive deflection rotation of fins that gives positive roll angle when looked from rear[18].

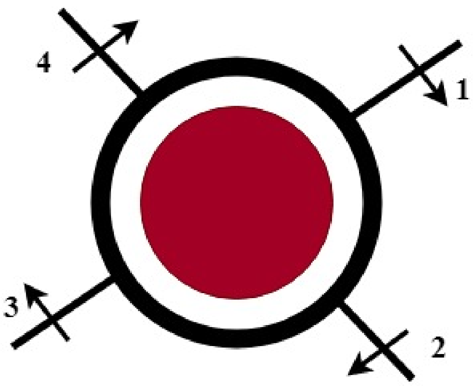

Figure 3.5: "X" Configuration of control surfaces

When looking from back, the deflection angles which result in positive roll motion states the positive deflection angles that are expressed with arrows. To roll the missile to the right or left, all four control surfaces deflects with the same angle. Pitch is to make the missile descend or climb. If 1 and 2 have +, 3 and 4 have - deflections then the missile shows pitch-up maneuver. If the opposite sign deflections occur the the missile shows pitch-down maneuver. Yaw is the turning of the missile. If 1 and 4 have -, 2 and 3 have + deflections then the missile steers to right when looked from back. If the opposite sign deflections occur the missile steers to left. Fin deflections are named according to the fin number stated as $\delta_1, \delta_2, \delta_3, \delta_4$. These four fins cause three rotation motion on each body axis cumulatively called

δ_a = aileron deflection (cause roll motion)

δ_q = elevator deflection (cause pitch motion)

δ_r = rudder deflection (cause yaw motion)

These deflections are calculated from four fin deflections as follows

$$\begin{aligned}
\delta_a &= \frac{\delta_1 + \delta_2 + \delta_3 + \delta_4}{4} \\
\delta_q &= \frac{\delta_1 + \delta_2 - \delta_3 - \delta_4}{4} \\
\delta_r &= \frac{\delta_1 - \delta_2 - \delta_3 + \delta_4}{4}
\end{aligned} \tag{3.13}$$

The integrated guidance-control system has the task of stabilizing the missile airframe while meeting the terminal conditions required for successful target interception. the first step in the design process is the definition of the control chains. In the pitch and yaw axis, the fin deflections are used to generate pitch and yaw rates, which in turn generate the angle of attack and angle of side-slip. The angle of attack and angle of side-slip then influence the line-of-sight rates.

3.3.4 Control Actuation System Model

Control actuation system is basically a motor system that actuates fins. It has its own closed loop control mechanism which takes autopilot fin commands as input and reacts on the system with its output according to its command tracking performance. Its dynamics can be stated as a second order linear system shown below[18].

$$\frac{\delta(s)}{\delta_c(s)} = \frac{\omega_n^2}{s^2 + 2\zeta\omega_n s + \omega_n^2} \tag{3.14}$$

where:

$\omega_n = natural frequency(rad = s)$

$\zeta = damping ratio$

Practically these systems have a rotation rate limit and also another limit comes from missile fin deflection angle limit. Where the lifting performance starts to decrease, i.e., control effectiveness, determines this deflection limit. Fin motor model or generally called control actuation system model is shown as follows.

$$\frac{d}{dt}\begin{bmatrix}\delta(t)\\ \dot{\delta}(t)\end{bmatrix} = \begin{bmatrix}0 & 1\\ -\omega_n^2 & -2\zeta\omega_n^2\end{bmatrix}\begin{bmatrix}\delta(t)\\ \dot{\delta}(t)\end{bmatrix} + \begin{bmatrix}0\\ \omega_n^2\end{bmatrix}\delta_c(t)$$

3.4 Two/Three dimensional Missile-Target Engagement

Figure 3.6 shows the basic parameters and geometry associated with the two dimensional missile/target engagement problem and the parameters are defined below[19].

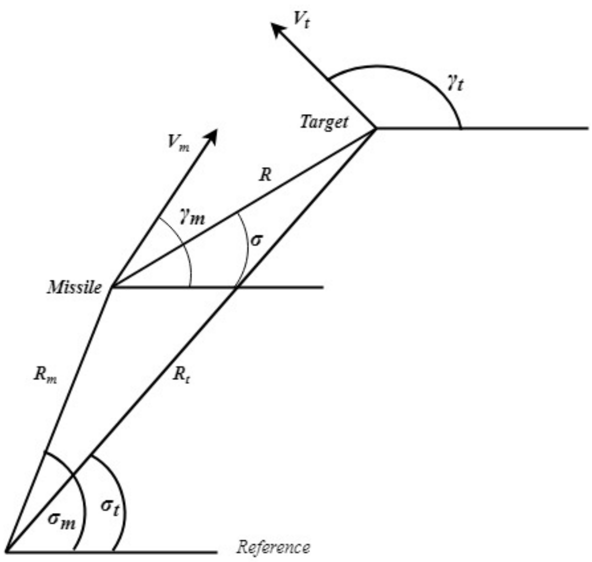

Figure 3.6: Missile/Target Geometry

V_t = Target Velocity

V_m = Missile Velocity

γ_t = Target flight path angle

γ_m = Missile flight path angle

R = Missile to Target range

R_t = Target Range

R_m = Missile Range

σ = Line Of angle

σ_t = Target line of sight angle

σ_m = Missile line of sight angle

3.4.1 Constant Bearing course

Figure 3.7 depicts the constant bearing course idea. As long as there is a positive closing velocity between the missile and the target, the constant bearing course will ensure an intercept. Proportional navigation uses the constant bearing course idea by driving the line of sight rate ,$\dot{\sigma}$, to zero. A constant bearing course is one where the line of sight between the target and the missile maintains a constant orientation in space.

3.4.2 Proportional navigation scheme

Figure 3.8 depicts the basic proportional navigation scheme. Assuming that the seeker head of the missile follows the target, the transverse acceleration perpendicular to the line of sight will equal the acceleration of the R vector in that direction. Mathematically, the acceleration of R is:

$$A_R = (\ddot{R} + \omega \times \omega \times R)i_R + (2\omega \times \dot{R} \times R + \dot{\omega} \times R)i_\sigma \tag{3.15}$$

Where:

R = Missile/Target line of sight vector.

$\dot{R}$ = Closing rate along R.

$\ddot{R}$ = Acceleration along R.

ω = Angular rate of change of R in inertial space.

A_m = Missile Acceleration perpendicular to R.

A_t = target Acceleration perpendicular to R.

A_R = Overall Acceleration of R.

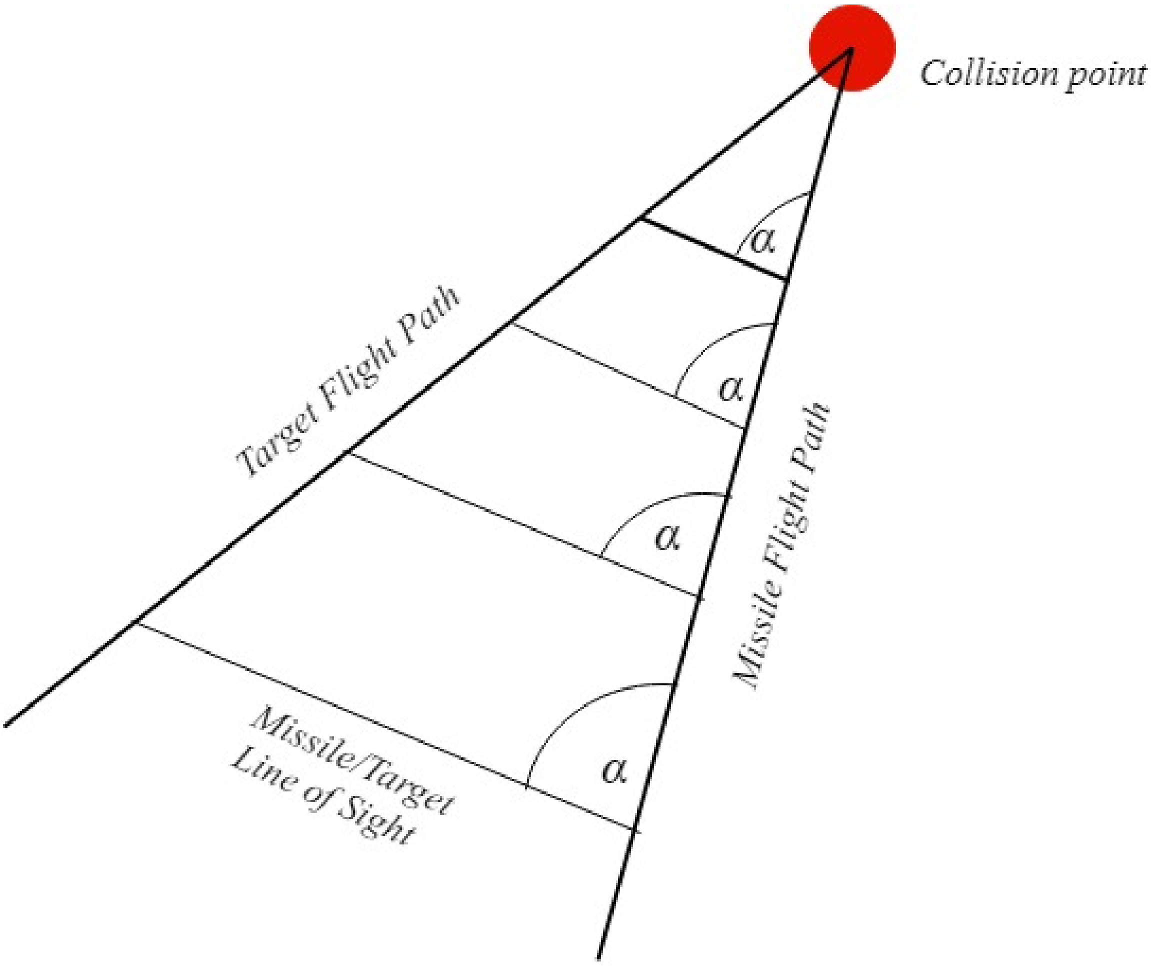

Figure 3.7: Constant Bearing Course

At this point a missile acceleration ,A_m, equal to the target acceleration ,A_t, will make the line of sight parallel to its original direction. As long as $\dot{R}$ remains along $R(\omega = 0)$ missile/target impact is assured.So, the transverse acceleration command is:

$$A_t - A_m = \dot{\omega} \times R + 2(\omega \times \dot{R}) \tag{3.16}$$

Assuming the line of sight rate is equal to the angular rate of change of R in inertial space, equation (3.16) now becomes:

$$A_t - A_m = R\ddot{\sigma} + 2\dot{R}\dot{\sigma} \tag{3.17}$$

3.4.3 Missile And Target Geometry

Velocity Relationship

Figure 3.9 shows the vectorial relationship of the missile and target velocity. From this figure

$$V_m = \sqrt{V_{mx}^2 + V_{my}^2 + V_{mz}^2}$$

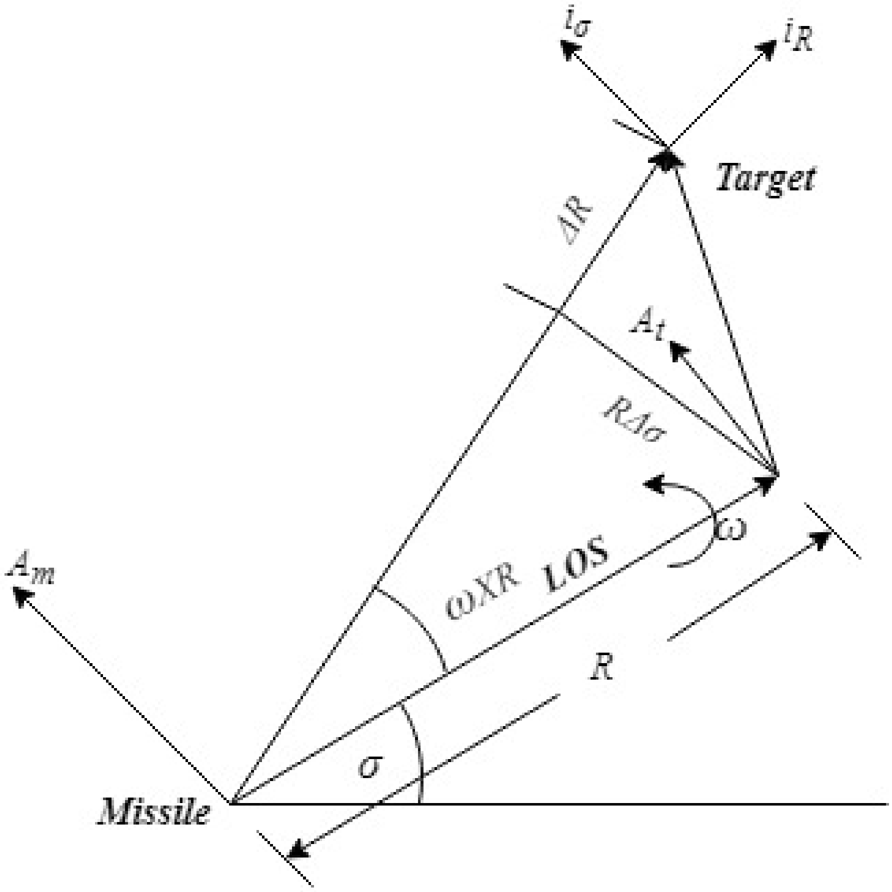

Figure 3.8: Vectorial Proportional Navigation Scheme

and

$$V_t = \sqrt{V_{tx}^2 + V_{ty}^2 + V_{tz}^2}$$

Line of Sight Angles

Given the target and missile position in Cartesian coordinates the line of sight angles are defined as

$$\begin{aligned} \sigma_{pitch} &= tan^{-1}\left[(z_t - z_m)/\sqrt{(x_t - x_m)^2 + (y_t - y_m)^2}\right] \\ \sigma_{yaw} &= tan^{-1}[(y_t - y_m)/(x_t - x_m)] \end{aligned} \tag{3.18}$$

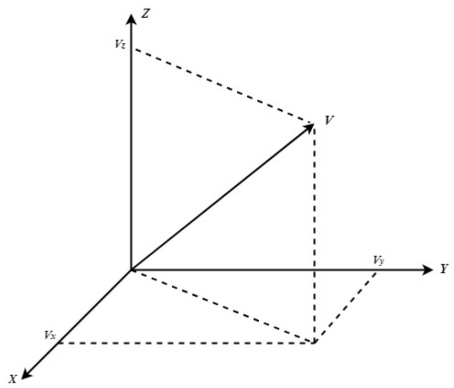

Figure 3.9: Velocity Relationship

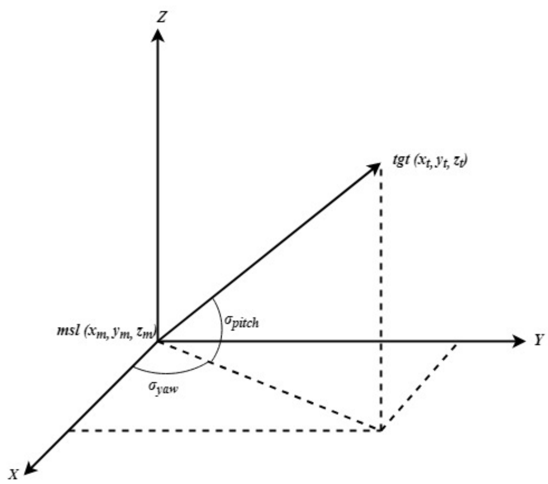

Figure 3.10: Pitch and Yaw Line of sight angle definitions

Figure 3.11 shows the target and missile line of sight angle definitions and these angles are expressed mathematically as

$$\begin{aligned} \sigma_{m\_pitch} &= tan^{-1}\left[z_m/\sqrt{x_m^2+y_m^2}\right] \\ \sigma_{m\_yaw} &= tan^{-1}[y_m/x_m] \\ \sigma_{t\_pitch} &= tan^{-1}\left[z_t/\sqrt{x_t^2+y_t^2}\right] \\ \sigma_{t\_yaw} &= tan^{-1}[y_t/x_t] \end{aligned} \tag{3.19}$$

The range vector (R) can be defined as

$$R = \sqrt{(x_t - x_m)^2 + (y_t - y_m)^2 + (z_t - z_m)^2} \tag{3.20}$$

The velocity components can be found from the Euler angle transformation.The x, y, and z directions are taken as the longitudinal, lateral, and normal axis of the missile, respectively. The corresponding angles that represent the angular displacements are ϕ (roll) ,θ(pitch) , and ψ(yaw). With the missile assumed to be roll stabilized, the roll angle will be taken as zero and not included. The Euler transformation matrix is given as

$$\begin{bmatrix} X \\ Y \\ Z \end{bmatrix} = \begin{bmatrix} cos(\theta)cos(\phi) & cos(\theta)sin(\phi) & -sin(\theta) \\ -sin(\phi) & cos(\phi) & 0 \\ sin(\theta)cos(\phi) & sin(\theta)sin(\phi) & cos(\theta) \end{bmatrix} \begin{bmatrix} I \\ J \\ K \end{bmatrix}$$

where I points north, J east, and K down. The transformation matrix represents the total transformation from the inertial coordinate system to the missile body axes.
From the above matrix, the linear components of the missiles velocity can be found using the fight path angles in the yaw and pitch planes[19].

$$\begin{aligned} V_{mx} &= V_m cos(\theta) cos(\phi) \\ V_{my} &= V_m cos(\theta) sin(\phi) \\ V_{mz} &= V_m(-sin(\theta)) \end{aligned} \tag{3.21}$$

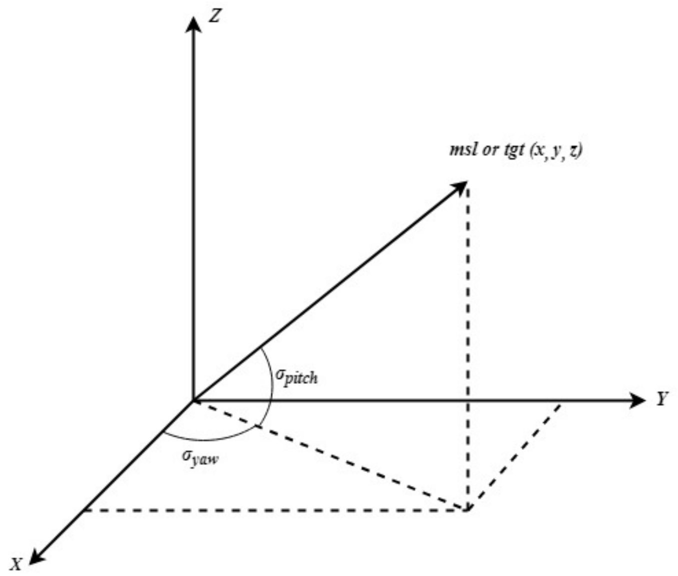

Figure 3.11: Target and Missile line of sight angle definitions

Flight Path Angles

The missile and target flight path angles are also defined in three dimensions. Figure 3.12 depicts the geometric definitions

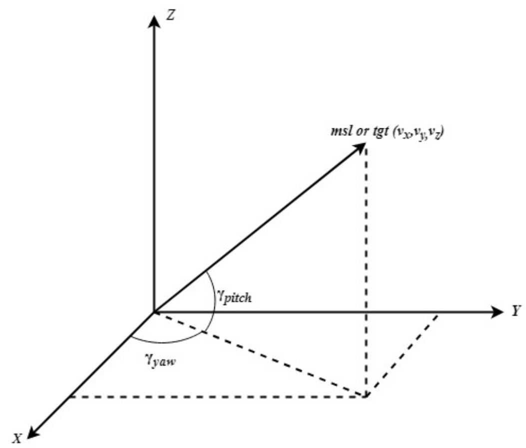

Figure 3.12: Target and Missile flight path angle definition

Mathematically,

$$
\begin{aligned}
\gamma_{m\_pitch} &= tan^{-1}\left[V_{mz}/\sqrt{V_{mx}^2+V_{my}^2}\right] \\
\gamma_{m\_yaw} &= tan^{-1}[V_{my}/V_{mx}] \\
\gamma_{t\_pitch} &= tan^{-1}\left[V_{tz}/\sqrt{V_{tx}^2+V_{ty}^2}\right] \\
\gamma_{t\_yaw} &= tan^{-1}[V_{ty}/V_{tx}]
\end{aligned}
\tag{3.22}
$$

Velocity and Acceleration in the pitch Plane

Figure 3.13 depicts the geometric definition of the pitch plane. Given the missile velocity, and the angles σ_{yaw} and γ_{m_yaw} ,the velocity in the pitch plane is

$$V_{m\_pitch} = V_m cos(\gamma_{m\_yaw} - \sigma_{yaw}) \tag{3.23}$$

From the basic relationship for the missile acceleration the missile pitch acceleration

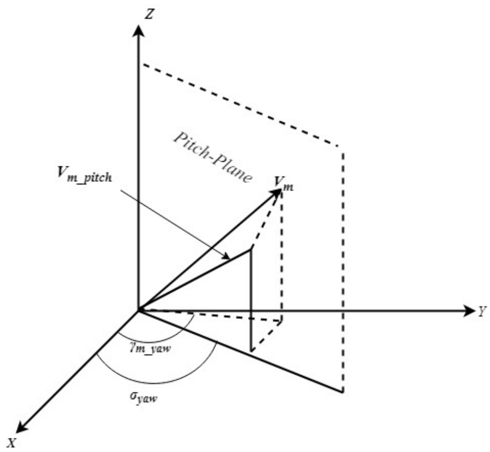

Figure 3.13: Pitch plane definition

is defined as

$$A_{m\_pitch} = V_{m\_pitch}.\dot{\gamma}_{m\_pitch} \tag{3.24}$$

This acceleration vector is then broken down into Cartesian coordinate system components. Assuming that the pitch acceleration vector is perpendicular to the vertical line of sight vector between the missile and target, Figure 3.14 shows the orientation of the acceleration components.

From this figure the following relationships are obtained

$$
\begin{aligned}
\ddot{x}_{m\_pitch} &= -(A_{m\_pitch}.sin\sigma_{pitch})cos\sigma_{yaw} \\
\ddot{y}_{m\_pitch} &= -(A_{m\_pitch}.sin\sigma_{pitch})sin\sigma_{yaw} \\
\ddot{z}_{m\_pitch} &= A_{m\_pitch}.cos\sigma_{pitch}
\end{aligned}
\tag{3.25}
$$

Velocity and acceleration in the Yaw Plane

The missile yaw plane is depicted in Figure 3.15. Given the missile velocity and the angle γ_{m_pitch}, the velocity in the yaw plane is

$$V_{m\_yaw} = V_m.cos\gamma_{m\_pitch} \tag{3.26}$$

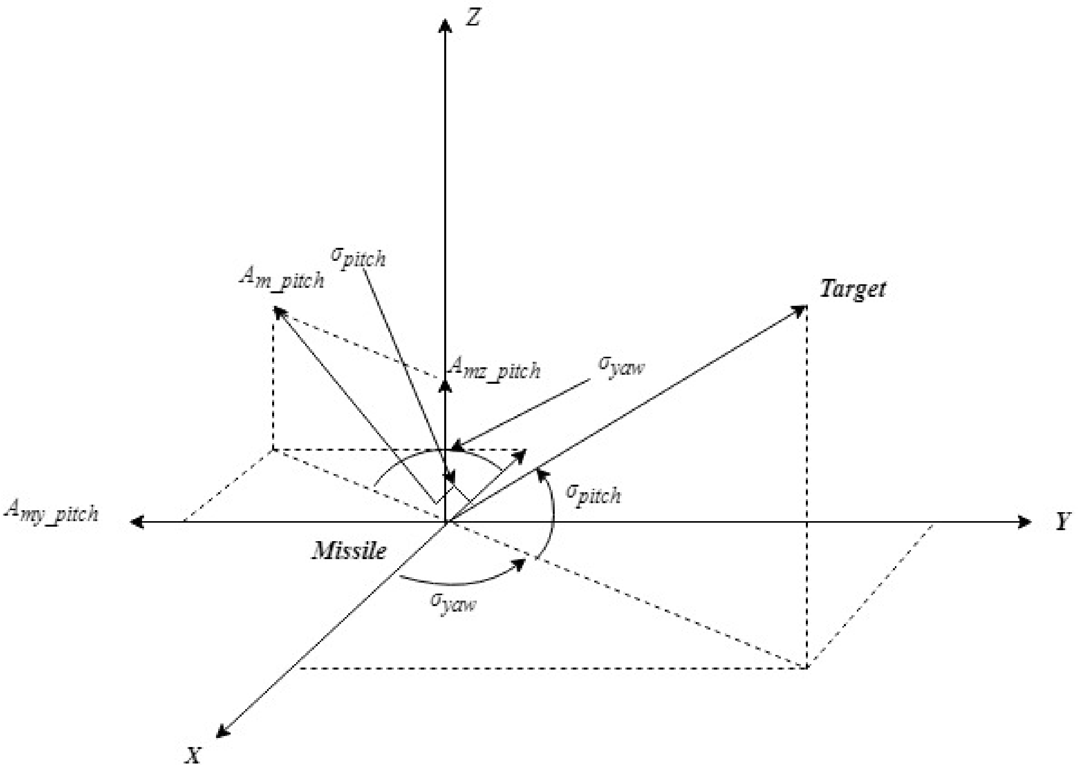

Figure 3.14: Pitch plane acceleration components

Again, from the basic missile acceleration relationship, the missile yaw acceleration is defined as

$$A_{m\_yaw} = V_{m\_yaw}.\dot{\gamma}_{m\_yaw} \tag{3.27}$$

The missile yaw acceleration components arc depicted in figure 3.16 and are given mathematically as

$$\begin{aligned} \ddot{x}_{m\_yaw} &= -A_{m\_yaw}.sin\sigma_{yaw} \\ \ddot{y}_{m\_yaw} &= A_{m\_yaw}.cos\sigma_{yaw} \end{aligned} \tag{3.28}$$

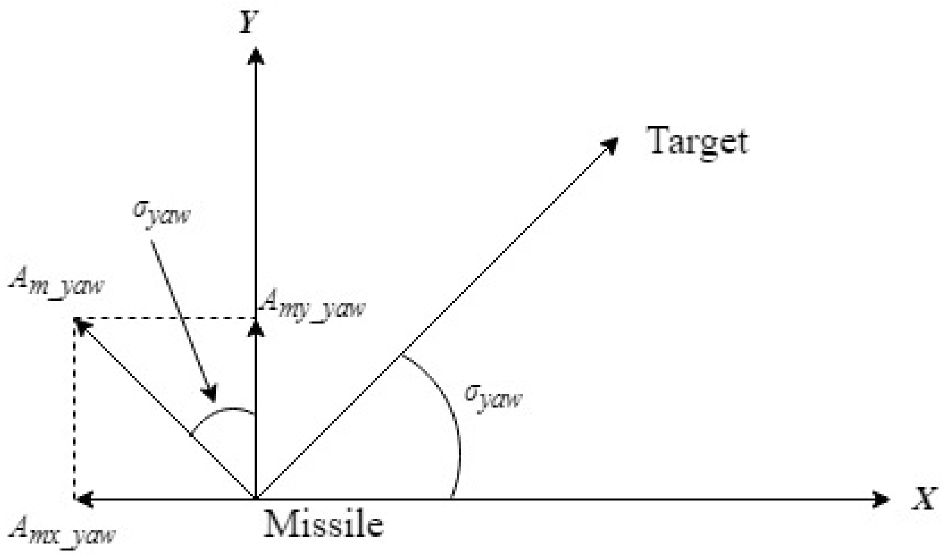

Figure 3.16: Yaw Plane Acceleration components

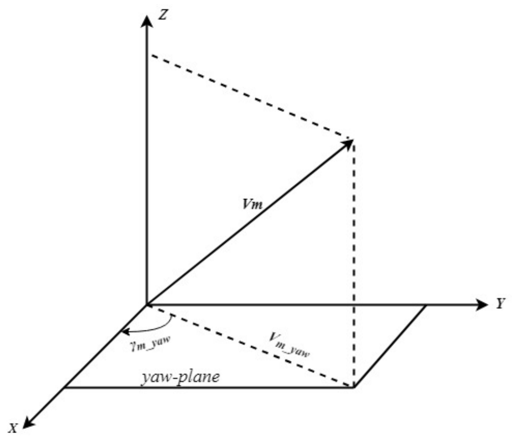

Figure 3.15: Yaw Plane definition

Total Missile Acceleration Components

Given the missile acceleration components in both the pitch and yaw planes, the total missile acceleration components are

$$\begin{aligned} \ddot{x}_m &= \ddot{x}_{m\_pitch} + \ddot{x}_{m\_yaw} \\ \ddot{y}_m &= \ddot{y}_{m\_pitch} + \ddot{y}_{m\_yaw} \\ \ddot{z}_m &= \ddot{z}_{m\_pitch} \end{aligned} \tag{3.29}$$

Finally, the total missile acceleration is

$$A_m = \sqrt{\ddot{x}_m^2 + \ddot{y}_m^2 + \ddot{z}_m^2} \tag{3.30}$$

Target Acceleration Components

The overall target acceleration is

$$A_t = \sqrt{\ddot{x}_t^2 + \ddot{y}_t^2 + \ddot{z}_t^2} \tag{3.31}$$

Closing Velocity and Time to go

the velocity of the target in the pitch plane is

$$V_{t\_pitch} = V_t cos(\gamma_{t\_yaw} - \sigma_{yaw})$$

The range rate, $\dot{R}$, is found by projecting the missile and target pitch plane velocities along the vertical line of sight from the missile to the target. Mathematically

$$\dot{R} = V_{t\_pitch}.cos(\gamma_{t\_pitch} - \sigma_{pitch}) - V_{m\_pitch}.cos(\gamma_{m\_pitch} - \sigma_{pitch}) \tag{3.32}$$

Knowing that the range rate is the negative of the closing velocity, the time to go is

$$t_{go} = \frac{R}{V_{closing}} = \frac{R}{-\dot{R}} \tag{3.33}$$

Where R is the range from the missile to the target. And t_{go} is the time to go.

Chapter 4

Sliding Mode Integrated Guidance and control Development

Integrated guidance and control (IGC) design is an emerging trend in missile technology. This is a response to meet the need for improving the accuracy of interceptors and extend their kill envelope. Current and past practices in industry have been to design guidance and control systems separately and then integrate them to form the complete missile. The whole system usually consists of a range of technologies from classical control theory to optimal estimation and control. These subsystems typically had different bandwidths. Despite the fact that this paradigm has been applied successfully on many systems, it can be argued that the overall system performance can be improved if the design exploits the synergy between the various missile subsystems. Furthermore, an IGC design will eliminate the number of iterations needed in the separate guidance-control design[1].

This approach exploits the finite time reaching phase of the sliding mode technique to ensure a desired constraint will be achieved in a finite time. The SMIGC approach used in this thesis is adapted form the article "Sliding mode integrated missile guidance and control"[20]. The selection of sliding variable to realize the intercept strategy is subject to the designer and can be any function of the state variables. In this thesis Sliding surfaces are chosen as the predicted impact point (PIP) heading errors in the vertical and horizontal planes. Heading error is defined as the error in missile heading from a collision course. When analyzing the Integrated Guidance and Control problem from a velocity-based point-of-view, the heading error becomes a very natural guidance parameter. Once the heading error is zero, the missile is on a collision course with the predicted impact point(PIP) and a hit is guaranteed. Next, SMIGC uses Terminal Second-Order Sliding Mode approach to remove chattering and guarantee the heading error is sent to zero in a finite time.

4.1 Intercept Geometry and Location of Predicted Impact Point

The new Integrated Guidance and Control(IGC) formulation steers the missile toward a fixed point in space, the Predicted Impact Point(PIP), which will minimize

the final miss distance. In order for the IGC formulation to work effectively, the PIP needs to be calculated with a high degree of accuracy.
The PIP is a virtual point that is created by projecting the targets position to some later point in time, and gives an indication of where the missile and the target will collide[1]. When the missile is correctly traveling toward the PIP, there exists a collision triangle, which is depicted in Figure 4.1. In this configuration, the distance traveled by the missile, d_m, in a certain period of time, t_{go}, will cause the missile to reach the same point as the target, which has traveled a distance dt in the same period of time. The current range between the missile and target is r.

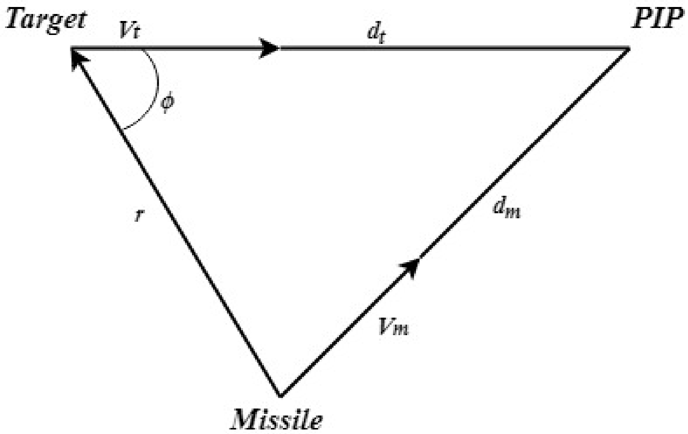

Figure 4.1: Collision Triangle Geometry

Figure 4.2 and Figure 4.3 contain sketches of the PIP geometry for the vertical (α) and horizontal (β) planes and detail how these two heading errors are defined. Note that as the target accelerates, the PIP location will be continuously changing. In order to direct the missile towards the PIP, the sliding mode approach sends the PIP heading errors, δ_α and δ_β, to zero in a finite time[1],[20].

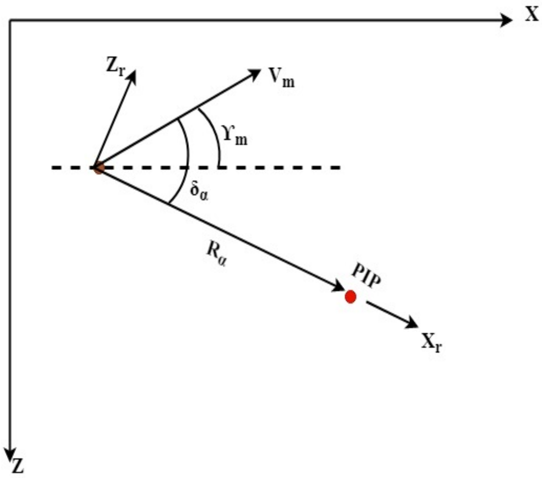

Figure 4.2: α-plane Geometry

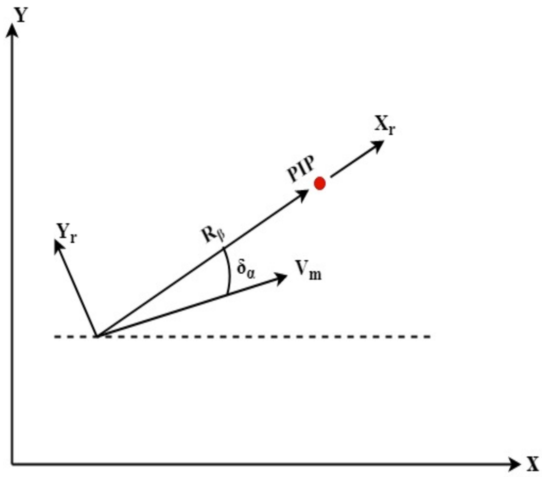

Figure 4.3: β-plane Geometry

4.2 Effect of Target Acceleration on the PIP Heading Error

It is assumed that the target can only accelerate normal to its direction of motion. Consequently, the target velocity direction can change but not its magnitude. Let the components of the targets normal acceleration in the α and β planes be taken as $A_{t\alpha}$ and $A_{t\beta}$ respectively. In terms of these normal acceleration components, the target acceleration vector can be expressed in the inertial $X-Y-Z$ frame as

$$a_{tgt} = [A_{t\alpha} sin\gamma_t + A_{t\beta} sin\phi_t]X + A_{t\beta} cos\phi_t Y + A_{t\alpha} cos\gamma_t Z \tag{4.1}$$

where γ_t and ϕ_t are the targets flight path angle and heading angle respectively. Now, the expression for the rate of change of the PIP location can be found as

$$\dot{r}_{PIP} = a_{tgt} t_{go} - v_{tgt}.\frac{(r_{pip} - r_{msl}).a_{tgt} t_{go}}{(r_{pip} - r_{msl}).V_{rel}} \tag{4.2}$$

where

$$r_{pip} = r_{tgt} + V_{tgt} t_{go} \tag{4.3}$$

$$V_{rel} = V_{tgt} - V_{msl} \tag{4.4}$$

and t_{go} is the time-to-go
substituting equations (4.1), (4.3),and (4.4) into equation (4.2) and carrying out the required vector operations equation (4.2) becomes[1]

$$\begin{aligned} \dot{r}_{PIP} = [(t_{go} sin\gamma_t - (A/C)\dot{x}_t)A_{ta} + (t_{go} sin\phi_t - (B/C)\dot{x}_t)A_{t\beta}]X + \\ [-(A/C)\dot{y}_t A_{ta} - (t_{go} cos\phi_t + (B/C)\dot{y}_t)A_{t\beta}]Y + \\ [(-t_{go} cos\gamma_t - (A/C)\dot{z}_t)A_{ta} + (-(B/C)\dot{z}_t)A_{t\beta}]Z \end{aligned} \tag{4.5}$$

where

$$A = (x_t - x_m + \dot{x}_t t_{go}) t_{go} sin\gamma_t - (z_t - z_m + \dot{z} t_{go}) t_{go} cos\gamma_t \tag{4.6}$$

$$B = (x_t - x_m + \dot{x}_t t_{go}) t_{go} sin\phi_t - (y_t - y_m + \dot{y}_t t_g o) t_{go} cos\phi_t \tag{4.7}$$

$$\begin{aligned} C = (x_t - x_m + \dot{x}_t t_{go})(\dot{x}_t - \dot{x_m}) + (y_t - y_m + \dot{y}_t t_{go})(\dot{y}_t - \dot{y_m}) + \\ (z_t - z_m + \dot{z}_t t_{go})(\dot{z}_t - \dot{z_m}) \end{aligned} \tag{4.8}$$

equation(4.5) shows that in the case of a non-maneuvering target the PIP location will remain constant. Next, it is desired to see the effect of target acceleration on the derivatives of the two heading errors, $\dot{\delta_\alpha}$ and $\dot{\delta_\beta}$. Without proof, these derivatives can be found to be[20]

$$\dot{\delta_\alpha} = (V_m/R_\alpha) sin\delta_\alpha + k_{N\alpha}\alpha + \frac{(\dot{r}_{PIP}.Z_r)}{R_\alpha} \tag{4.9}$$

$$\dot{\delta_\beta} = (V_m/R_\beta) sin\delta_\beta + k_{Y\beta}\beta + \frac{(\dot{r}_{PIP}.Y_r)}{R_\beta} \tag{4.10}$$

where the $\hat{z_r}$ and $\hat{y_r}$ axes are as defined in figure 4.2. The third terms in equations (4.9) and (4.10) account for the effect of the target normal acceleration on the rate of change of the heading errors through equation (4.5). In order to simplify equations (4.9) and (4.10), note that

$$Z_r = -sin(\gamma_m - \delta_\alpha)\hat{X} + cos(\gamma_m - \delta_\alpha)\hat{Z} \tag{4.11}$$

$$Y_r = -sin(\phi_m - \delta_\beta)\hat{X} + cos(\phi_m - \delta_\beta)\hat{Y} \tag{4.12}$$

substituting equations(4.5),(4.11)and (4.12) into equations (4.9)and (4.10) leads to

$$\dot{\delta}_\alpha = (V_m/R_\alpha)sin\delta_\alpha + k_{N\alpha}\alpha + (D/R_\alpha)A_{t\alpha} + (E/R_\alpha)A_{t\beta} \tag{4.13}$$

$$\dot{\delta}_\beta = (V_m/R_\beta)sin\delta_\beta + k_{Y\beta}\beta + (F/R_\beta)A_{t\alpha} + (G/R_\beta)A_{t\beta} \tag{4.14}$$

where

$$D = [-t_{go}sin\gamma_t + (A/C)\dot{x}_t]sin(\gamma_m - \delta_\alpha) - [t_{go}cos\gamma_t + (A/C)\dot{z}_t]cos(\gamma_m - \delta_\alpha) \tag{4.15}$$

$$E = [-t_{go}sin\phi_t + (B/C)\dot{x}_t]sin(\gamma_m - \delta_\alpha) - (B/C)\dot{z}_t cos(\gamma_m - \delta_\alpha) \tag{4.16}$$

$$F = [-t_{go}sin\gamma_t + (A/C)\dot{x}_t]sin(\phi_m - \delta_\beta) - (A/C)\dot{y}_t cos(\phi_m - \delta_\beta) \tag{4.17}$$

$$G = [-t_{go}sin\phi_t + (B/C)\dot{x}_t]sin(\phi_m - \delta_\beta) - [t_{go}cos\phi_t + (B/C)\dot{y}_t]cos(\phi_m - \delta_\beta) \tag{4.18}$$

Equations (4.13) and (4.14) are exact epressions for the effect of target acceleration on the α-plane and β-plane heading errors. Note the interesting result that a target acceleration in one of the two planes will actually affect the heading error in both planes. This is because a target maneuver in either of the planes will cause a change in motion along the X axis. The X axis is contained in both the vertical and horizontal planes, so a change in this axis will actually affect the perceived motion in both planes.

4.3 Sliding Mode Guidance and Control Analysis

4.3.1 Sliding Mode Control

Variable structure control (VSC) is a form of discontinuous nonlinear control. The method alters the dynamics of a nonlinear system by application of a high-frequency switching control. The state-feedback control law is not a continuous function of time; it switches from one smooth condition to another. So the structure of the control law varies based on the position of the state trajectory.
The main mode of VSC operation is sliding mode control (SMC). The concept of sliding mode control first appeared in Russian literature in the fifties of the twentieth

century. The former Soviet Union experts Emelyanov first proposed the concept of sliding mode variable structure[21]. Sliding Mode Control is a robust control design approach enabling to maintain stability and performance in the presence of modeling errors. For a system of the form $\dot{x} = f(x, u, t)$, SMC involves constraining the motion of the system to a sliding surface, or manifold, $s = 0$[1]. This surface is typically chosen such that a desirable system behavior is achieved. Once on this sliding surface, the system dynamics are restricted to the equations of the surface and are robust to matched plant uncertainties and external disturbances. The only requirement placed on uncertainties is that they be bounded, and that the bound is known beforehand. To keep the system on the sliding surface, an infinite switching control law is typically used.
The strengths of SMC include[22]:

- Low sensitivity to plant parameter uncertainty.
- Greatly reduced-order modeling of plant dynamics
- Finite-time convergence (due to discontinuous control law)
- Solution does not depend on plant parameters nor disturbance, and this is called invariance property.
- Its ability to globally stabilize the system

The weaknesses of SMC include:

- Chattering due to implementation imperfections, fast-switching of controller and discretization chatter due to the fixed sampling rate[22].

Solving a problem with Sliding Mode Control will generally involve two steps. First, a sliding surface (or surfaces) must be chosen for the system. This is a very important step, as the sliding surface ultimately defines how the system will behave. The second step is to develop a control law which will take the system from its initial state to the sliding surface (reaching phase), and then keep the system on that surface (sliding phase). Since the system will typically only exhibit the desired behavior once on the sliding surface, it is obviously important that the surface be reached in a finite time. In an ideal scenario, a system will converge exactly to the surface $s = 0$ and begin moving along it. However, this ideal case is based on the assumption that the control input can switch values at an infinite frequency. Control hardware will realistically only be able to operate at a finite frequency. Thus, in the real scenario the system will not reach the surface exactly and instead overshoot it by a small amount. The system will then try to converge back to the surface, overshoot again, and the process will be repeated. This behavior leads to a phenomenon called chattering, which is known for being fairly devastating on control hardware. In order to bypass this undesirable behavior when implementing a SMC approach, modifications are typically made that attempt to minimize or eliminate the chattering effect. This can be done by replacing the discontinuous signum function in the control law with a continuous saturation function, or by using a Higher-Order Sliding Mode (HOSM) approach[23].

4.3.2 First order Sliding Mode Control

It is known that the crucial and the most important step of SMC design is the construction of the sliding surface $s(t)$, also called sliding function, $s(t) \in R$,[21],[24],. Sliding mode is said first order sliding mode if and only if $s(t) = 0$ and $s(t)\dot{s}(t) < 0$. The inequality $s(t)\dot{s}(t) < 0$ is the fundamental condition for sliding mode [24]. The aim of the first-order sliding mode control is to force the state (error) to move on the switching surface $s(t) = 0$. The sliding surface, $s(t)$ in the traditional SMC depends on the tracking error, $e(t)$ and derivative(s) of the tracking error as [21],[24]:

$$s(t) = \left(\lambda_c + \frac{d}{dt}\right)^{n-1} e(t)$$

where n denotes order of uncontrolled system, λ_c is a positive constant, $\lambda_c \in R^+$. If the system concerned is assumed to be of second-order ($n = 2$), and then, in two-dimensional phase plane related to above equation, the solution is a straight line passing through the origin.Maintaining the error on $s(t)$ will result in $e(t)$ approaching zero. Therefore, $s(t) = 0$ is a stable sliding surface and $e(t) \to 0$ as $t \to \infty$. If the error has reached the sliding surface $s(t) = 0$, then it simultaneously slides into the origin $e(t) = 0$ despite the matched parametric uncertainties and disturbances. The error starting from a certain initial value will converge to the boundary layer and move inside the boundary layer towards the horizontal axis until it reaches $\dot{e}(t) = 0$.

4.3.3 Higher order Sliding Mode Control (HOSM)

A sliding mode is said r^{th} order sliding mode if and only if $s(t) = \dot{s}(t) = ... = s^{r-1}(t) = 0$.It is well-known that first-order sliding mode approaches can only be utilized when the sliding surface has a relative degree of 1. To handle problems with larger relative degrees, a higher-order sliding mode (HOSM) approach must be used. In high-order sliding mode control, the purpose is to force the state (error) to move on the switching surface $s(t) = 0$ and to keep its $(r - 1)$ first successive derivatives null [21]. In the particular case of the second-order sliding mode control, the controller's aim is to steer to zero not only the sliding surface $s(t)$ but also its first-order time derivative as $s(t) = \dot{s}(t) = 0$ [25], [26]. The problem of interest in the present case is to generate a second-order sliding mode on a chosen sliding surface $s(t)$.

4.3.4 Terminal Second-Order Sliding Mode Control Law (TSM)

This control law was first developed in [27], where it was utilized for approach and landing guidance of a reentry vehicle. The approach leads to a terminal control law in that it is utilized to guarantee a certain constraint (the sliding surface) is satisfied only at the final time. Contrary to many current approaches to Higher Order Sliding Mode control, Terminal Sliding Mode focuses on the finite time reaching phase of sliding mode rather than on the sliding phase[27], [28]. The main advantage of Terminal Sliding Mode is that it allows the user to shape the trajectory the system follows to reach the sliding surface through the use of a tuning constant. By shaping the trajectory, it is possible to find a solution which takes the system to the surface while satisfying various performance criteria.

Assume that it is desired to reach a sliding surface of the form

$$s = f(x) = 0$$

and that the first two time derivatives of the surface are

$$\dot{s} = h(x)$$
$$\ddot{s} = l(x) + \rho + g(x)u$$

The functions $h(x), l(x)$ and $g(x)$ are assumed to be known functions of x, and ρ is assumed to be a bounded uncertainty term. It can be seen that the control input u appears in the second derivative of the sliding surface, so the surface has a relative degree of 2. The goal is to find an expression for u such that the sliding surface and its derivative will both go to zero at some desired finite time tr. This goal is achieved through the use of a backstepping approach, where $\dot{s}$ is taken as a virtual control input [27]. In order to find the value of $\dot{s}$ that would be needed to send s to zero, a candidate Lyapunov function, V_l , is chosen as

$$V_l = \frac{1}{2}s^2$$

Taking the time derivative of V_l leads to

$$\dot{V}_l = s\dot{s}$$

In order to guarantee that the surface s will go to zero in a finite time, $\dot{s}$ must be chosen such that the Lyapunov functions derivative $\dot{V}_l$ is negative-definite. This negative-definite property can be achieved by choosing $\dot{s}$ as

$$\dot{s} = -\frac{ns}{t_r - t}, n > 1$$

where t_r is a desired reaching time. Substituting equations it is found that

$$\dot{V}_l = -\frac{ns^2}{t_r - t}$$

It can be simplified to

$$\dot{V}_l = -\frac{2nV_l}{t_r - t}$$

$\dot{V}_l$ can now be analytically integrated from the initial condition, $(V(t_0), t_0)$ to a later point in time $(V(t), t)$, leading to the solution

$$V_l(t) = \frac{V_l(t_0)}{(t_r - t_0)^{2n}}(t_r - t)^{2n}$$

Note that if n is greater than 0.5, the $(t_r - t)^{2n}$ in the equation goes to zero as t approaches t_r. Thus, as long as this condition on n is satisfied the Lyapunov function (and thus the sliding surface) is guaranteed to go to zero at the desired reaching time t_r. Also, $\dot{s}$ is adaptive in that it depends on the instantaneous values of the sliding surface and the time t. The equation $\dot{s} = -\frac{ns}{t_r - t}, n > 1$, essentially defines a desired trajectory for the sliding surfaces derivative to follow. This condition will not necessarily be met at the initial time, as the initial value of $\dot{s}$ depends entirely on the initial conditions of the problem. Thus, the control input u must be used to send $\dot{s}$ from its initial value to the trajectory defined by $\dot{s} = -\frac{ns}{t_r - t}, n > 1$ in a finite time, and then keep $\dot{s}$ on that trajectory. Since the system must perform some movement along the trajectory to guarantee that s and $\dot{s}$ will go to zero, it is important that the trajectory be reached some finite amount of time before the reaching time t_r. One way to guarantee that the trajectory will be reached in a finite time is to consider $\dot{s} = -\frac{ns}{t_r - t}, n > 1$ as a new sliding surface

$$s_2 = \dot{s} + \frac{ns}{t_r - t} = 0$$

The time derivative of the new surface can then be found as

$$\dot{s}_2 = l(x) + \frac{n\dot{s}(t_r - t) + ns}{(t_r - t)^2} + \rho + g(x)u$$

It can be seen from the above equation that the new sliding surface s_2 has a relative degree of one with respect to the control input u.
To find an expression for u that will send s_2 to zero in some finite time , a candidate Lyapunov function is chosen as

$$V_l = \frac{1}{2}s_2^2$$

Differentiating this leads to

$$\dot{V}_l = s_2\dot{s}_2 = s_2\left[l(x) + \frac{n\dot{s}(t_r - t) + ns}{(t_r - t)^2} + \rho + g(x)u\right]$$

In order to guarantee the Lyapunov function reaches zero in a finite time, u is selected as

$$u = -\frac{1}{g(x)}\left[l(x) + \frac{n\dot{s}(t_r - t) + ns}{(t_r - t)^2} + (\eta + |\rho_{max}|)sgn\left(\dot{s} + \frac{ns}{t_r - t}\right)\right]$$

It can be shown that with the control law u the Lyapunov functions derivative satisfies the condition

$$\dot{V}_l < -\eta|s_2|$$

The parameter η is a positive constant that is used to guarantee that the surface s_2 will go to zero. Also, $|\rho_{max}|$ is the known bound of the uncertainty term ρ. The Terminal Sliding Mode control law which solves the above control problem is summarized in the following theorem (derived in [27]) :
Theorem 1: Suppose a sliding surface $s = f(x)$ has a relative degree of two, with a second derivative of the form $\ddot{s} = l(x) + \rho + g(x)u$. Then, using the control law

$$u = -\frac{1}{g(x)}\left[l(x) + \frac{n\dot{s}(t_r - t) + ns}{(t_r - t)^2} + (\eta + |\rho_{max}|)sgn\left(\dot{s} + \frac{ns}{t_r - t}\right)\right]$$

where η is an appropriately chosen positive constant, ρ_{max} is the known bound of the uncertainty term ρ, and $n > 1$, it can be guaranteed that s and $\dot{s}$ will go to zero in the finite time t_r.
The control law above is a useful result in that it guarantees the sliding surface and its derivative will go to zero at some chosen finite time t_r.
Furthermore by adjusting the tuning constant n, it is possible to shape the trajectory

the system follows to the sliding surface in order to satisfy various performance criteria. However, it should be noted that this control law cannot be used to maintain the system on the surface s = 0 after it has been reached (i.e. when $t > t_r$). The TSM control law is ideally meant to be used for applications where the problem is essentially over once the sliding surface is reached. Finally, it should also be noted that the control law above can be modified for systems with arbitrary relative degrees in a very straightforward fashion.

4.3.5 Alpha-Plane Guidance and Control

Recall from Equation 4.13 that the derivative of the heading error in the α-plane is

$$\dot{\delta}_\alpha = (V_m/R_\alpha)sin\delta_\alpha + k_{N\alpha}\alpha + (D/R_\alpha)A_{t\alpha} + (E/R_\alpha)A_{t\beta}$$

Now noting that the derivatives of the angle of attack and pitch rate q are given by[20]:

$$\dot{\alpha} = -k_{N_\alpha} + q \tag{4.19}$$

$$\dot{q} = k_{m_\alpha} + k_{m_\delta}\delta_q \tag{4.20}$$

and making the assumption that the target acceleration does not affect higher-order derivatives of the heading error, Equation 4.13 can be differentiated until the pitch fin deflection δ_q appears, leading to

$$\ddot{\delta}_\alpha = (V_m/R_\alpha)^2 sin(2\delta_\alpha) + (V_m/R_\alpha)cos\delta_\alpha k_{N_\alpha}\alpha + k_{N_\alpha}(q - k_{N_\alpha}\alpha) + \rho_1 \tag{4.21}$$

$$\begin{aligned}\dddot{\delta}_\alpha &= 2(V_m/R_\alpha)^3 sin(3\delta_\alpha) + 3(V_m/R_\alpha)^2 cos(2\delta_\alpha)k_{N_\alpha}\alpha - (V_m/R_\alpha)sin\delta_\alpha k_{N_\alpha}^2\alpha^2 \\ &+(V_m/R_\alpha)cos\delta_\alpha k_{N_\alpha}(q - k_{N_\alpha}\alpha) + k_{N_\alpha}[k_{M_\alpha}\alpha + k_{M_\delta}\delta_q - k_{N_\alpha}(q - k_{N_\alpha}\alpha)] + \rho_2\end{aligned} \tag{4.22}$$

where ρ_1 and ρ_2 are uncertainty terms caused by differentiation of the unknown target acceleration. These two uncertainty terms are assumed to be unknown but bounded. It can be seen from equation 4.22 that the fin deflection appears in the third derivative of the heading error.

It is now desired to derive an expression for the pitch fin deflection δ_q that will send the heading error δ_α to zero in a finite time. A sliding mode approach is used by choosing a sliding surface s_α as

$$s_\alpha = \delta_\alpha = 0 \tag{4.23}$$

It can be seen that if the sliding surface in equation 4.23 is reached, the heading error δ_α will be zero and an impact with the target will be achieved. Next, the sliding surface 4.23 is differentiated until the fin deflection δ_q appears as

$$\begin{aligned}\dot{s} &= \dot{\delta}_\alpha \\ \ddot{s} &= \ddot{\delta}_\alpha \\ \ddot{s} = \dddot{\delta}_\alpha &= H + \rho_2 + I\delta_q\end{aligned} \tag{4.24}$$

where

$$\begin{aligned}H &= 2(V_m/R_\alpha)^3 sin(3\delta_\alpha) + 3(V_m/R_\alpha)^2 cos(2\delta_\alpha)k_{N_\alpha}\alpha - (V_m/R_\alpha)sin\delta_\alpha k_{N_\alpha}^2\alpha^2 \\ &+(V_m/R_\alpha)cos\delta_\alpha k_{N_\alpha}(q - k_{N_\alpha}\alpha) + k_{N_\alpha}[k_{M_\alpha}\alpha + k_{M_\delta}\delta_q - k_{N_\alpha}(q - k_{N_\alpha}\alpha)]\end{aligned} \tag{4.25}$$

$$I = k_{N_\alpha} k_{m_\delta} \tag{4.26}$$

From equation 4.24 it is noted that the fin deflection appears in the third derivative of the sliding surface, implying that the surface has a relative degree of three. The objective is to now develop an expression for the fin deflection that will guarantee the sliding surface and its first two derivatives go to zero in a desired finite time. However, note that in order to guarantee a hit with the target the heading error only needs to be zero at the time of impact. While maintaining a zero heading error for a certain amount of time before impact also guarantees a hit, it is not requirement. Sending the heading error to zero earlier rather than later can actually lead to much larger fin deflections. The system therefore is not necessarily required to be maintained on the sliding surface; the system only needs to be on the surface at impact. Thus, the TSM control law presented in [27] can be utilized to solve this problem.
Recall from theorem 1

$$u = -\frac{1}{g(x)}\left[l(x) + \frac{n\dot{s}(t_r - t) + ns}{(t_r - t)^2} + (\eta + |\rho_{max}|)sgn\left(\dot{s} + \frac{ns}{t_r - t}\right)\right]$$

The fin deflection control law can be found as

$$\begin{aligned} \delta_q = -\frac{1}{I}\Bigg[H + \frac{2n\ddot{\delta}_\alpha t_{go}^2 + n(n+3)\dot{\delta}_\alpha t_{go} + 2n(n+1)\delta_\alpha}{t_{go}^3} + \\ (\eta + |\rho_{2,max}|)sgn\left(\frac{\ddot{\delta}_\alpha t_{go}^2 + 2n\delta_\alpha t_{go} + n(n+1)\delta_\alpha}{t_{go}^2}\right)\Bigg] \end{aligned} \tag{4.27}$$

4.3.6 Beta-Plane Guidance and Control

This section outlines the construction of an expression for the yaw fin deflection δ_r for control in the β-plane. The objective of the control law is to send the -plane heading error δ_β to zero in a finite time. Recall from equation 4.14 that the heading error derivative in the β-plane is[20]

$$\dot{\delta}_\beta = (V_m/R_\beta)sin\delta_\beta + k_{Y\beta}\beta + (F/R_\beta)A_{t\alpha} + (G/R_\beta)A_{t\beta}$$

Noting that the derivatives of the sideslip angle β and the yaw rate r are

$$\dot{\beta} = -k_{Y_\beta}\beta - r \tag{4.28}$$

$$\dot{r} = k_{n_\beta}\beta + k_{n_\delta}\delta_r \tag{4.29}$$

equation 4.18 is differentiated until the yaw fin deflection δ_r appears as

$$\ddot{\delta}_\beta = (V_m/R_\beta)^2 sin(2\delta_\beta) + (V_m/R_\beta)cos\delta_\beta k_{Y_\beta}\beta + k_{Y_\beta}(-r - k_{Y_\beta}\beta) + \rho_3 \tag{4.30}$$

$$\begin{aligned} \dddot{\delta}_\beta = 2(V_m/R_\beta)^3 sin(3\delta_\beta) + 3(V_m/R_\beta)^2 cos(2\delta_\beta)k_{Y_\beta}\beta - (V_m/R_\beta)sin\delta_\beta k_{Y_\beta}^2\beta^2 \\ +(V_m/R_\beta)cos\delta_\beta k_{Y_\beta}(-r - k_{Y_\beta}\beta) + k_{Y_\beta}[-k_{N_\beta}\beta - k_{N_\delta}\delta_r - k_{Y_\beta}(-r - k_{Y_\beta}\beta)] + \rho_4 \end{aligned} \tag{4.31}$$

where ρ_3 and ρ_4 are bounded uncertain terms caused by differentiating the target acceleration. As the heading error in the α-plane, the control input appears in the third derivative of δ_β. A sliding surface is now chosen as

$$s = \delta_\beta = 0 \tag{4.32}$$

which guarantees the heading error will go to zero. The sliding surface is differentiated until the fin deflection δ_r appears as

$$\begin{aligned} \dot{s} &= \dot{\delta}_\beta \\ \ddot{s} &= \ddot{\delta}_\beta \\ \dddot{s} = \dddot{\delta}_\beta &= J + \rho_4 + K\delta_r \end{aligned} \tag{4.33}$$

where

$$\begin{aligned} J = {} & 2(V_m/R_\beta)^3 sin(3\delta_\beta) + 3(V_m/R_\beta)^2 cos(2\delta_\beta) k_{Y_\beta}\beta - (V_m/R_\beta) sin\delta_\beta k_{Y_\beta}^2 \beta^2 \\ & + (V_m/R_\beta) cos\delta_\beta k_{Y_\beta}(-r - k_{Y_\beta}\beta) + k_{Y_\beta}[-k_{N_\beta}\beta - k_{N_\delta}\delta_r - k_{Y_\beta}(-r - k_{Y_\beta}\beta)] \end{aligned} \tag{4.34}$$

$$K = -k_{Y_\beta} k_{n_\delta} \tag{4.35}$$

The fin deflection δ_r is found in the third derivative of the sliding surface , so it has a relative degree of three. Now, as in the α-plane case, the objective is to solve for an expression for δ_r that will send the sliding surface and its first two derivatives to zero in a finite time. This is once again performed using the TSM approach from theorem 1, which yields a control law of the form

$$\begin{aligned} \delta_r = -\frac{1}{K} \Bigg[& J + \frac{2n\ddot{\delta}_\beta t_{go}^2 + n(n+3)\dot{\delta}_\beta t_{go} + 2n(n+1)\delta_\beta}{t_{go}^3} + \\ & (\eta + |\rho_{4,max}|) sgn\left(\frac{\ddot{\delta}_\beta t_{go}^2 + 2n\delta_\beta t_{go} + n(n+1)\delta_\beta}{t_{go}^2} \right) \Bigg] \end{aligned} \tag{4.36}$$

The control law in equation 4.36 guarantees that the heading error δ_β will go to zero at the time of impact.

Chapter 5

Simulation Studies

Through the accurately described kinematics of Missile target engagement and the model of dynamics of a missile, simulation can be developed. The integrated engagement model is developed by combining the state vector of missile target engagement kinematics and state vector of dynamics of a missile making new state vector creating algebraic relationships between state-variables and control inputs.

$[x_k] \rightarrow$ State vector of the missile target engagement kinematics.

$[x_M] \rightarrow$ State vector of the missile dynamics.

$$x = \begin{bmatrix} x_k & x_M \end{bmatrix}$$

$[x] \rightarrow$ The new state vector

The development shown above is for body based integrated guidance and control. But, This formulation was unable to accurately capture the physics behind missile motion[1]. A single loop Integrated Guidance and control is only achieved if a proper intercept strategy is used for interception. In this thesis interception is achieved by minimizing the final miss distance through fin deflection using velocity based integrated guidance and control formulation.

5.1 Airframe Simulation

Airframe simulation shows how the missile airframe responds when the tail is deflected. The geometric configuration parameters and material properties of the flexible missile are shown in table 5.1. A case was run for the generic missile in

Table 5.1: parameters and material properties of the missile

Mass	Diameter	Length	Material Density	Density	Young's Modulus
$400kg$	$0.12meter$	$4.0meter$	$7861.05kg/m^3$	$7.27g/cm^3$	$2.0 \times 10^{11}pascal$

which the missile fin was deflected $5°$ when the missile was at sea level traveling at $9.15m/s$. It can be seen from figure 5.1 that a $5°$ fin deflection in the positive direction causes the missile to build up to a negative angle of attack. The buildup in angle of attack enables the missile to accelerate.

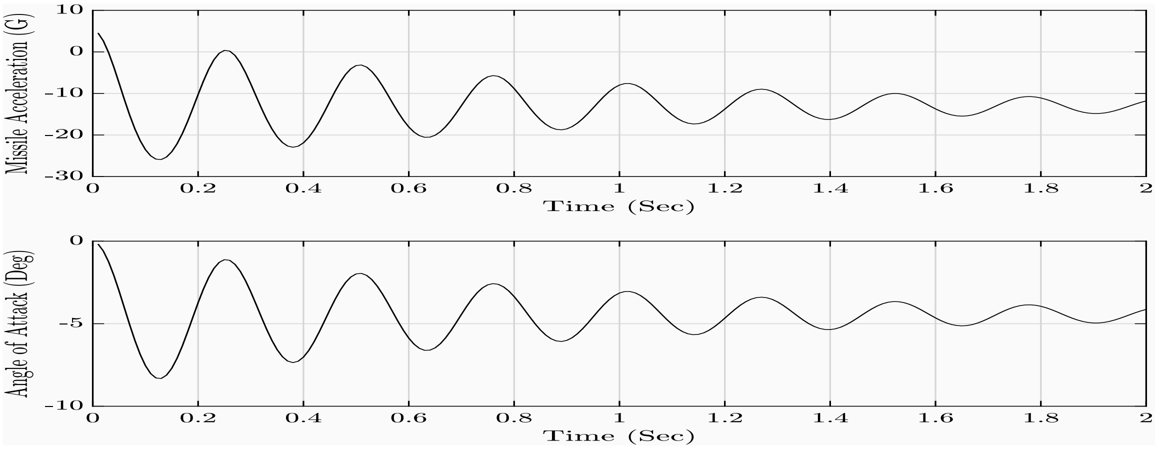

Figure 5.1: A 5° fin deflection results in approximately −5° angle of attack

5.2 Missile-Target Engagement Simulations in Two/Three Dimensions

The missile-target engagement scenario consists of a missile attempting to intercept a target through acceleration changes. Different simulations are carried out on the proposed control techniques to ensure the developed controller drives the system along the desired manifold and achieves required performance. In Proportional navigation homing guidance method the rate of flight-path angle of the interceptor is made proportional with a navigation ratio N to the rate of turn of the LOS between the interceptor and the target. The missile vector is defined as the missile's spatial and velocity components, namely:

$$X_m = \begin{bmatrix} x_m \\ \dot{x}_m \\ y_m \\ \dot{y}_m \\ z_m \\ \dot{z}_m \end{bmatrix}$$

Thus the missile can be represented as:

$$\dot{X}_m = A_m X_m + B_m U_m$$

The control input matrix is:

$$U_m = \begin{bmatrix} \ddot{x}_m \\ \ddot{y}_m \\ \ddot{z}_m \end{bmatrix}$$

Thus the A and B matrices can be written as follows:

$$A_m = \begin{bmatrix} 0 & 1 & 0 & 0 & 0 & 0 \\ 0 & 0 & 0 & 0 & 0 & 0 \\ 0 & 0 & 0 & 1 & 0 & 0 \\ 0 & 0 & 0 & 0 & 0 & 0 \\ 0 & 0 & 0 & 0 & 0 & 1 \\ 0 & 0 & 0 & 0 & 0 & 0 \end{bmatrix}, B_m = \begin{bmatrix} 0 & 0 & 0 \\ 1 & 0 & 0 \\ 0 & 0 & 0 \\ 0 & 1 & 0 \\ 0 & 0 & 0 \\ 0 & 0 & 1 \end{bmatrix}$$

The target kinematics are derived in a similar fashion. The target can be described by a state equation, namely:

$$\dot{X}_t = A_t X_t + B_t U_t$$

where:

$$X_t = \begin{bmatrix} x_t \\ \dot{x}_t \\ y_t \\ \dot{y}_t \\ z_t \\ \dot{z}_t \end{bmatrix}, U_t = \begin{bmatrix} \ddot{x}_t \\ \ddot{y}_t \\ \ddot{z}_t \end{bmatrix}$$

$$A_t = \begin{bmatrix} 0 & 1 & 0 & 0 & 0 & 0 \\ 0 & 0 & 0 & 0 & 0 & 0 \\ 0 & 0 & 0 & 1 & 0 & 0 \\ 0 & 0 & 0 & 0 & 0 & 0 \\ 0 & 0 & 0 & 0 & 0 & 1 \\ 0 & 0 & 0 & 0 & 0 & 0 \end{bmatrix}, B_t = \begin{bmatrix} 0 & 0 & 0 \\ 1 & 0 & 0 \\ 0 & 0 & 0 \\ 0 & 1 & 0 \\ 0 & 0 & 0 \\ 0 & 0 & 1 \end{bmatrix}$$

The target dynamic equations are defined with respect to the trajectory it follows; for example if the target is at level flight the accelerations are zero and so is the control matrix. The scenario is conducted for different initial conditions and with different target maneuvers.

For a continuous time state-space system described by the following set of equations

$$\dot{X}(t) = AX(t) + BU(t)$$

$$\dot{Y}(t) = CX(t) + DU(t)$$

a transformation into a discrete time system, with a T time interval, can be achieved:

$$X(k+1) = \Phi X(k) + \Gamma U(k)$$

$$Y(k) = CX(k) + DU(k)$$

according to the transformation equations:

$$\Phi = e^{At}$$

$$\Gamma = \left[\int_0^T e^{At} dt \right] B$$

One way of calculating the matrix exponent is:

$$e^{AT} = \mathcal{L}^{-1}[(SI - A)^{-1}]\big|_{t=T} = I + AT + \frac{A^2T^2}{2!} + \frac{A^3T^3}{3!} + ...$$

As the proportional navigation method the objective can be transferred into designing the control input δ_q and δ_r[29]. PN can be expressed as $\dot{\gamma}_m = c_0\dot{\lambda}$.

where:

$\dot{\gamma}_m \rightarrow$ the rate of flight-path angle of the missile.

$\dot{\lambda} \rightarrow$ the rate of turn of the Line of sight between the missile and the target.

$c_0 \rightarrow$ a positive constant.

Substituting $n_L = V\dot{\gamma}_m$ yields $n_L = c_0 V\dot{\lambda}$. Then design control inputs δ_q and δ_r to make $n_L \rightarrow c_0 V\dot{\lambda}$ in each plane.

Assumptions

1. A skid-to-turn roll-stabilized missile is considered. The motion of such a missile can be separated into two perpendicular channels, thus allowing to treat only a planar motion.
2. The missiles and targets deviations from the collision triangle are small during the end-game.
3. Material density is constant throughout the body and the steel was chosen for modeling.
4. The missile thrust exactly cancels drag.
5. The orientation of the missile can be described by the Euler angles that represent the flight path angles in pitch and yaw.
6. The seeker head angle rate is a good estimate of the line-of -sight rate.
7. For small angles of attack and side-slip, the velocity vector is assumed to be aligned with the body center line.
8. A uniform circular cross section is assumed.
9. The missile's weight is assumed constant. .
10. The missile is limited to 20 g's in either plane.
11. The target is capable of instantaneous acceleration.
12. The target is limited to a maximum of 8.0 g's.
13. The maximum missile speed is 900 meter per second.
14. The maximum target speed is 500 per second.
15. The missile is pointed toward the target at launch.

Scenario 1: A Constant Velocity Target

Target at Steady, Level Flight

The simulation is initially conducted with the missile engaging a constant velocity target. The initial conditions for this scenario are:

$$x_m(0) = 0m, y_m(0) = 0m, z_m(0) = 0m, V_{mx}(0) = 900m/s, V_{my}(0) = 0m/s, V_{mz}(0) = 0m/s,$$
$$x_t(0) = 9000m, y_t(0) = 0m, z_t(0) = 15, V_{tx}(0) = 300m/s, V_{ty}(0) = m/s, V_{tz}(0) = 0m/s$$

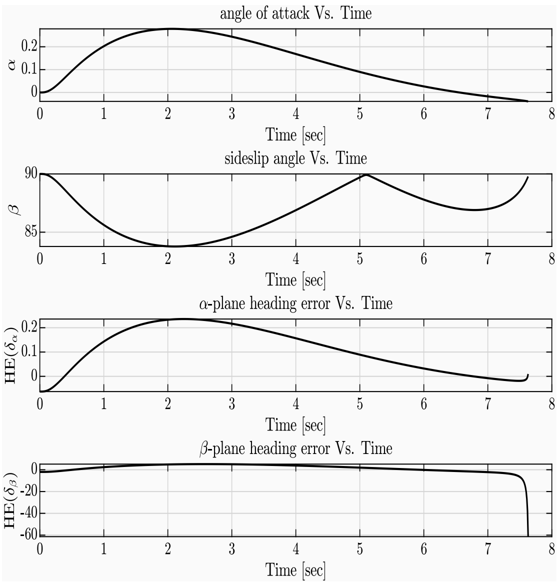

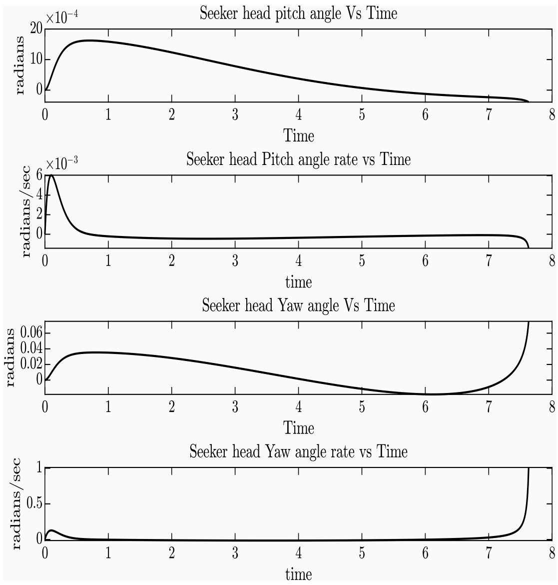

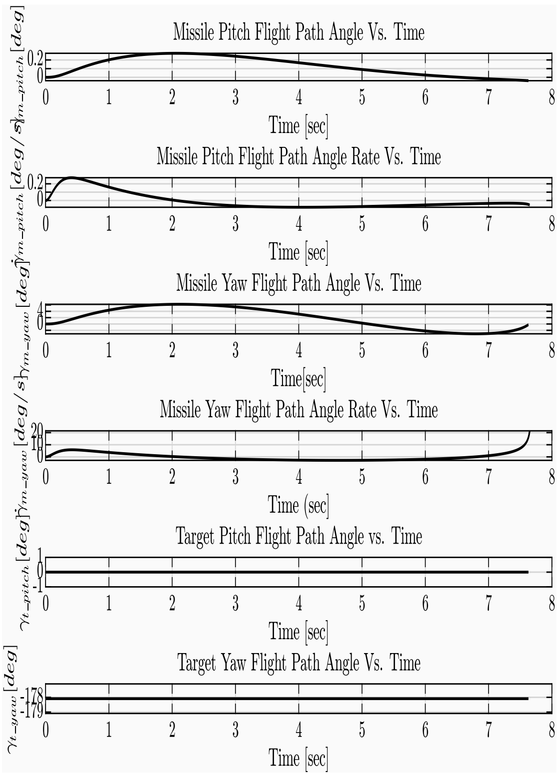

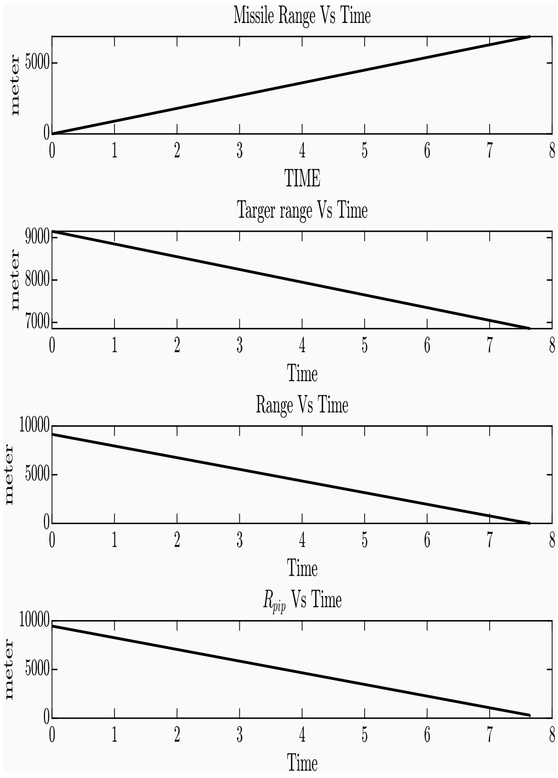

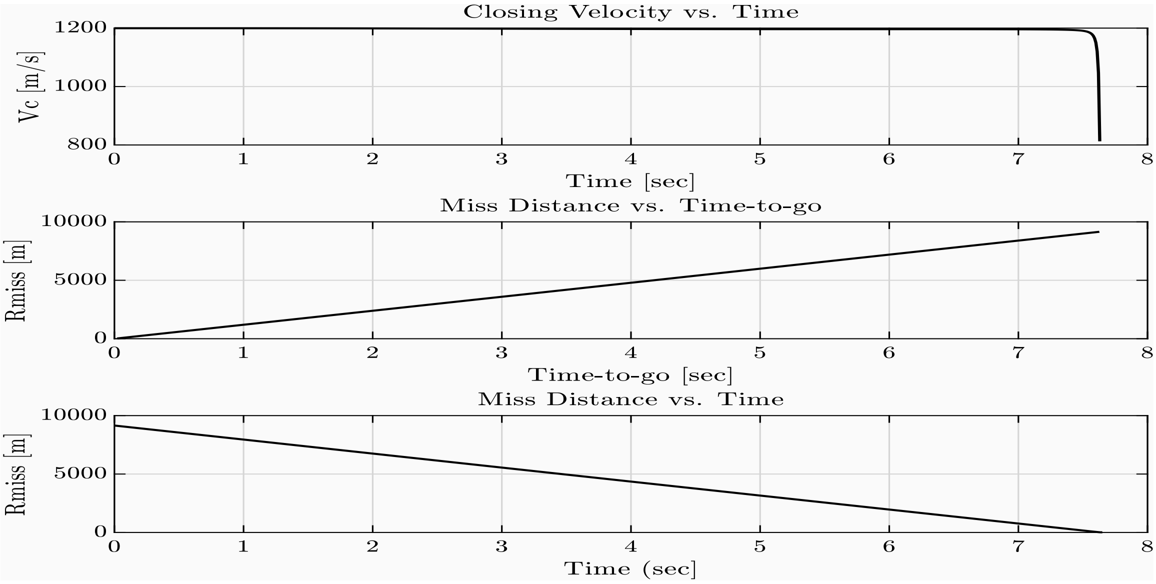
Closing Velocity vs. Time
Vc [m/s]
Time [sec]
Miss Distance vs. Time-to-go
Rmiss [m]
Time-to-go [sec]
Miss Distance vs. Time
Rmiss [m]
Time (sec)

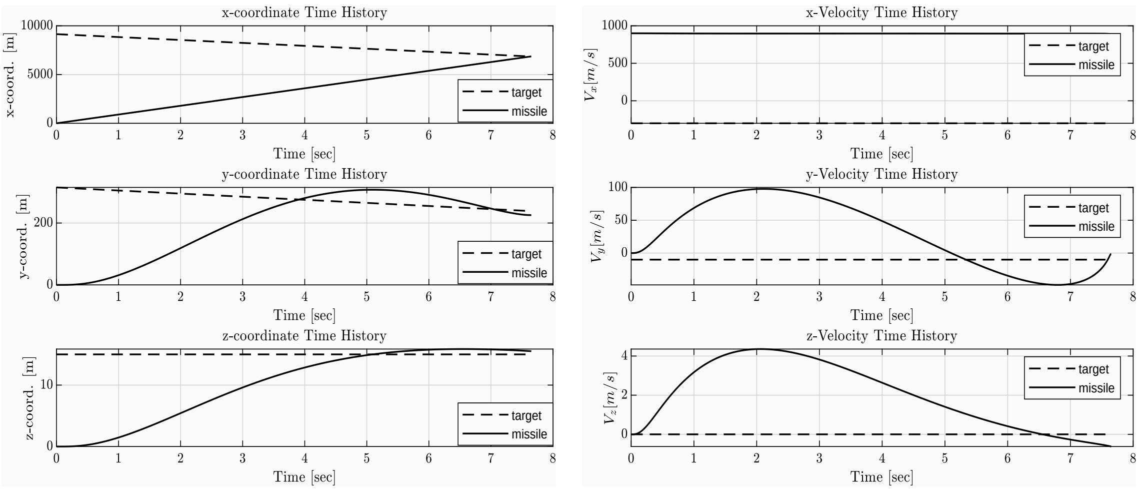
x-coordinate Time History
x-coord. [m]
y-coordinate Time History
y-coord. [m]
z-coordinate Time History
z-coord. [m]
x-Velocity Time History
y-Velocity Time History
z-Velocity Time History
target
missile
Time [sec]

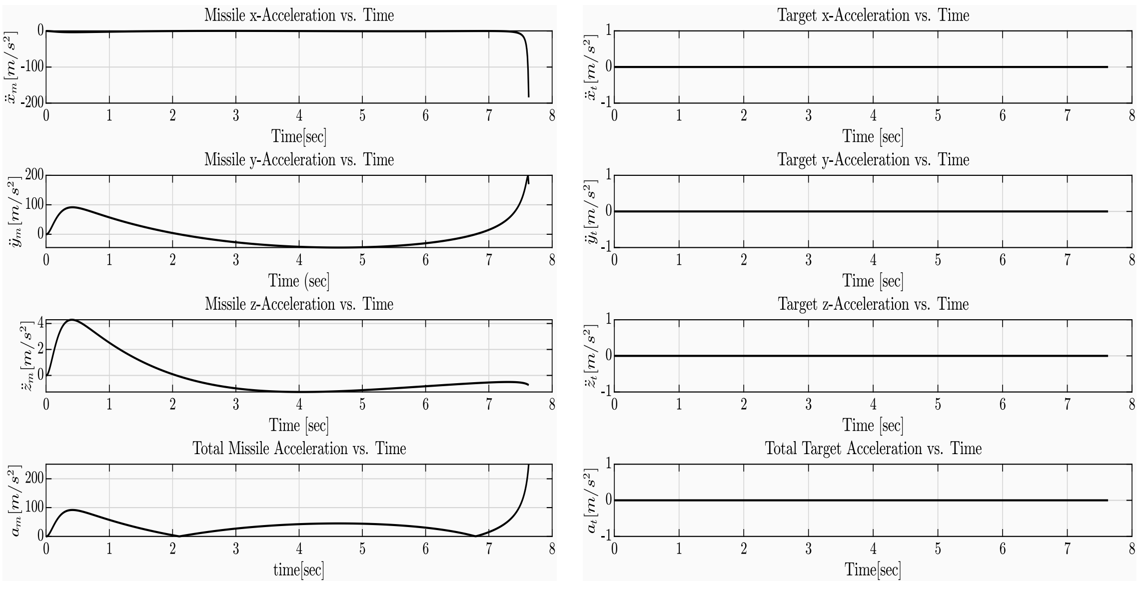
Missile x-Acceleration vs. Time
Missile y-Acceleration vs. Time
Missile z-Acceleration vs. Time
Total Missile Acceleration vs. Time
Target x-Acceleration vs. Time
Target y-Acceleration vs. Time
Target z-Acceleration vs. Time
Total Target Acceleration vs. Time
Time [sec]

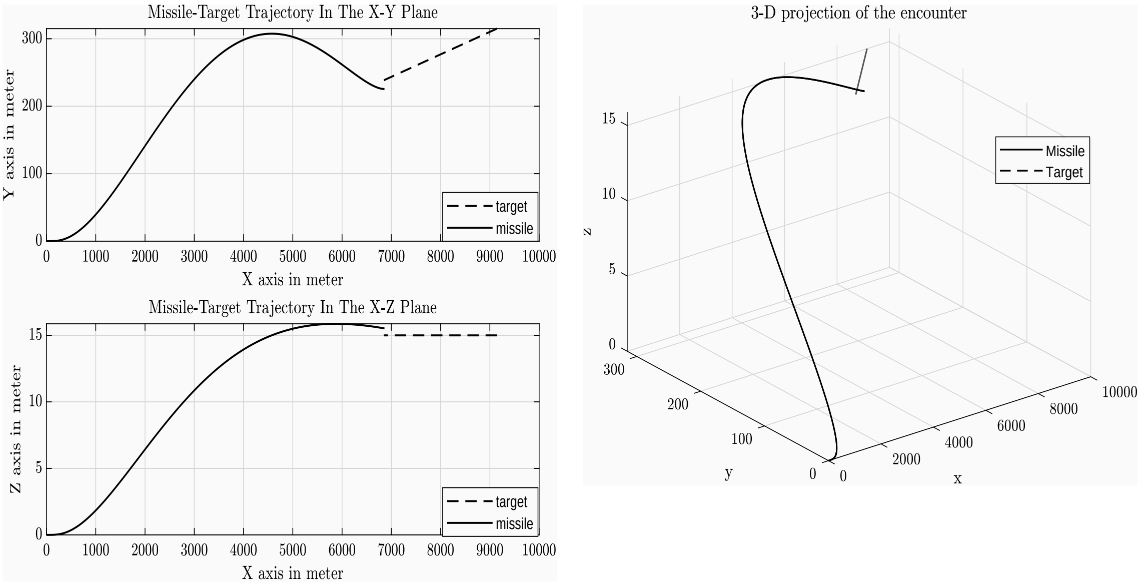

Figure 5.2: Constant velocity target scenario

Scenario 2: A Constant Acceleration Target

In this scenario, the target accelerates at a constant rate of 5 m/s^2 in the y direction. The initial conditions are:

$$x_m(0) = 0m, y_m(0) = 350m, z_m(0) = 0m, V_{mx}(0) = 650m/s, V_{my}(0) = 650m/s, V_{mz}(0) = 0m/s,$$
$$x_t(0) = 650, y_t(0) = 0m, z_t(0) = 150m, V_{tx}(0) = 0m/s, V_{ty}(0) = 300m/s, V_{tz}(0) = 0m/s,$$
$$a_{xt}(0) = 0m/s^2, a_{yt}(0) = 5m/s^2, a_{zt}(0) = 0m/s^2$$

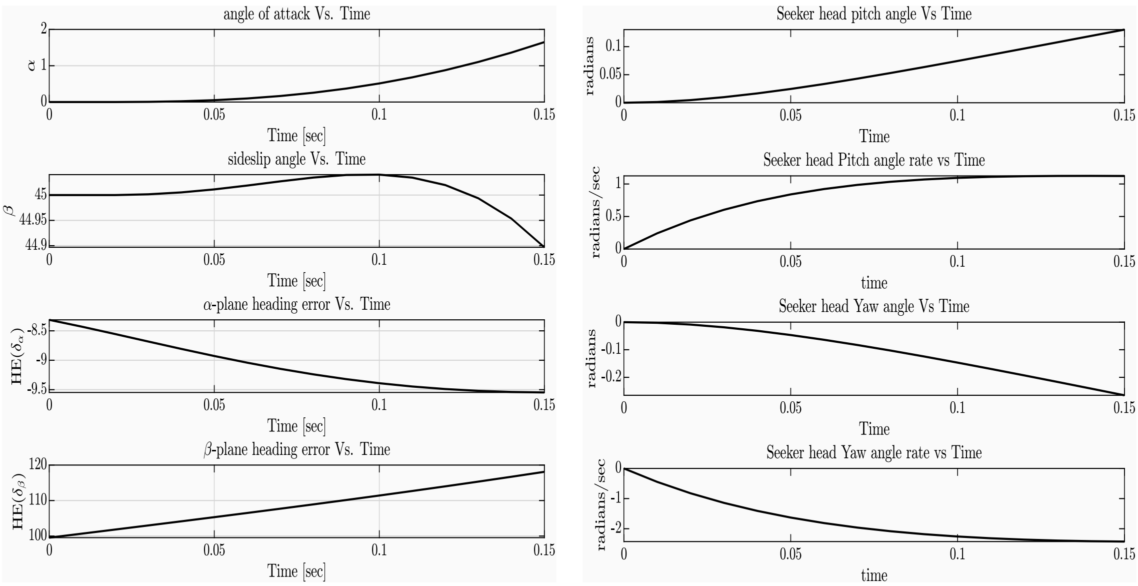

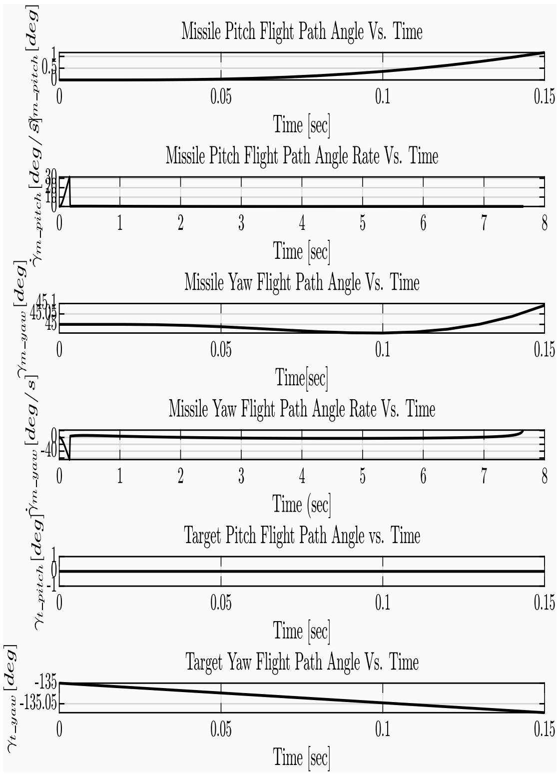
Missile Pitch Flight Path Angle Vs. Time
Time [sec]
Missile Pitch Flight Path Angle Rate Vs. Time
Time [sec]
Missile Yaw Flight Path Angle Vs. Time
Time[sec]
Missile Yaw Flight Path Angle Rate Vs. Time
Time (sec)
Target Pitch Flight Path Angle vs. Time
Time [sec]
Target Yaw Flight Path Angle Vs. Time
Time [sec]

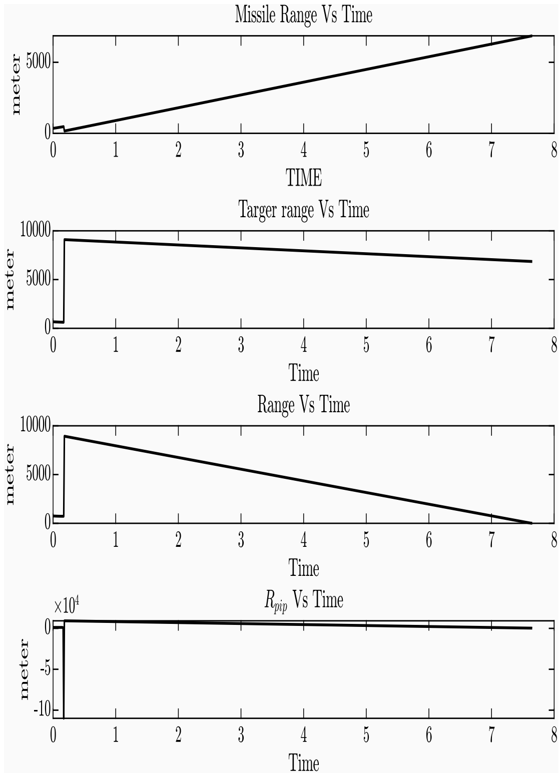
Missile Range Vs Time
meter
TIME
Targer range Vs Time
meter
Time
Range Vs Time
meter
Time
R_{pip} Vs Time
meter
Time

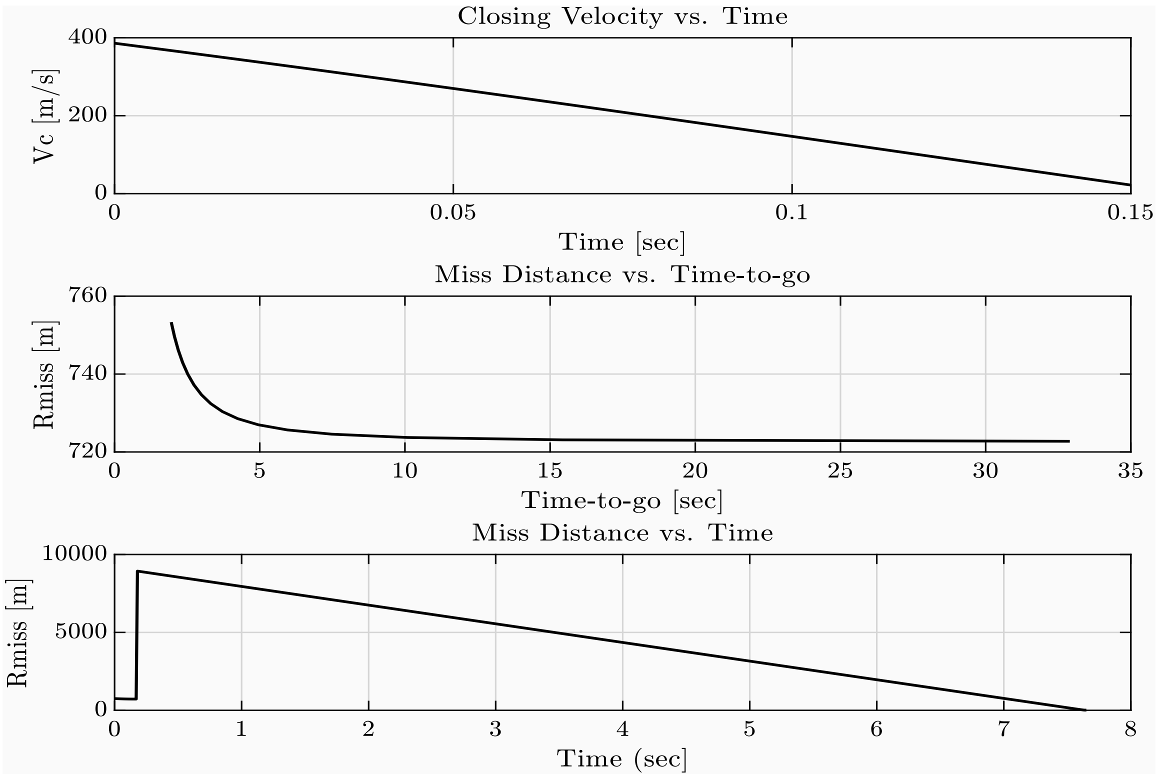
Closing Velocity vs. Time
Vc [m/s]
Time [sec]
Miss Distance vs. Time-to-go
Rmiss [m]
Time-to-go [sec]
Miss Distance vs. Time
Rmiss [m]
Time (sec)

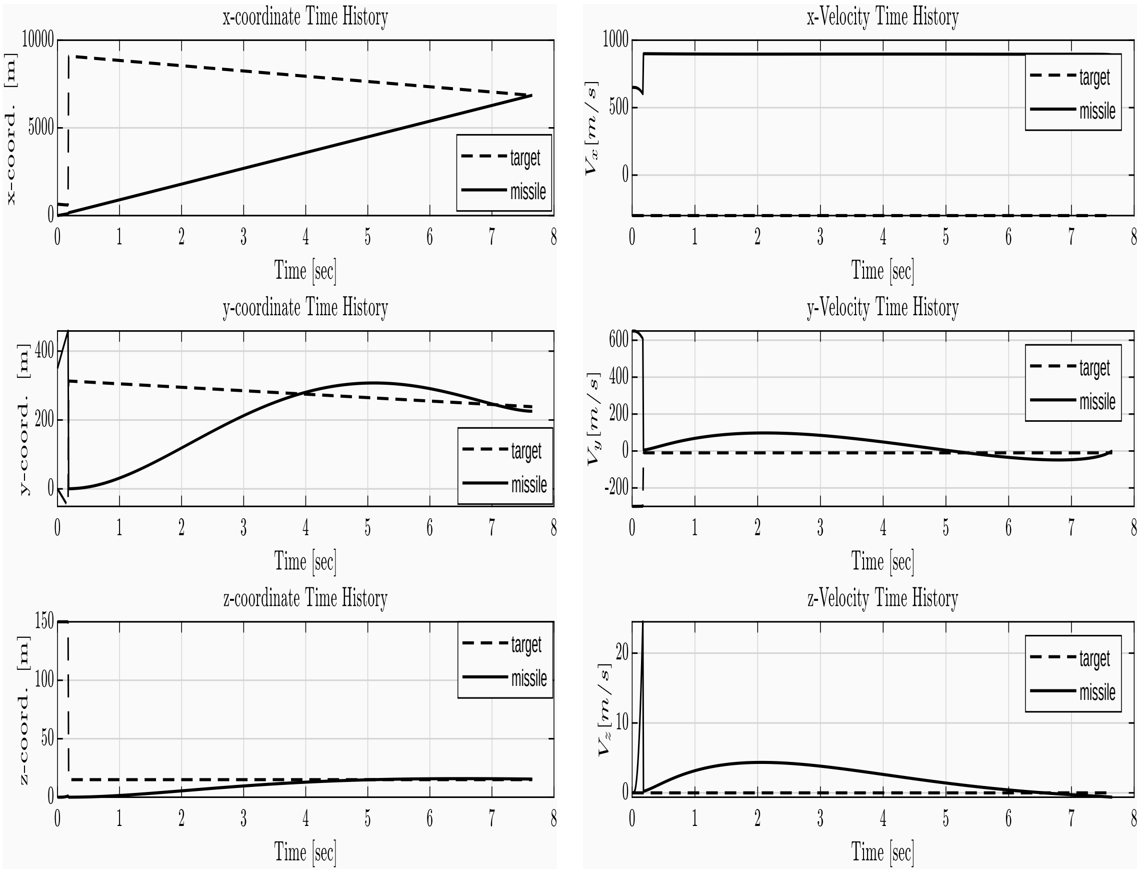
x-coordinate Time History
x-coord. [m]
Time [sec]
target
missile
x-Velocity Time History
$V_x[m/s]$
y-coordinate Time History
y-coord. [m]
y-Velocity Time History
$V_y[m/s]$
z-coordinate Time History
z-coord. [m]
z-Velocity Time History
$V_z[m/s]$

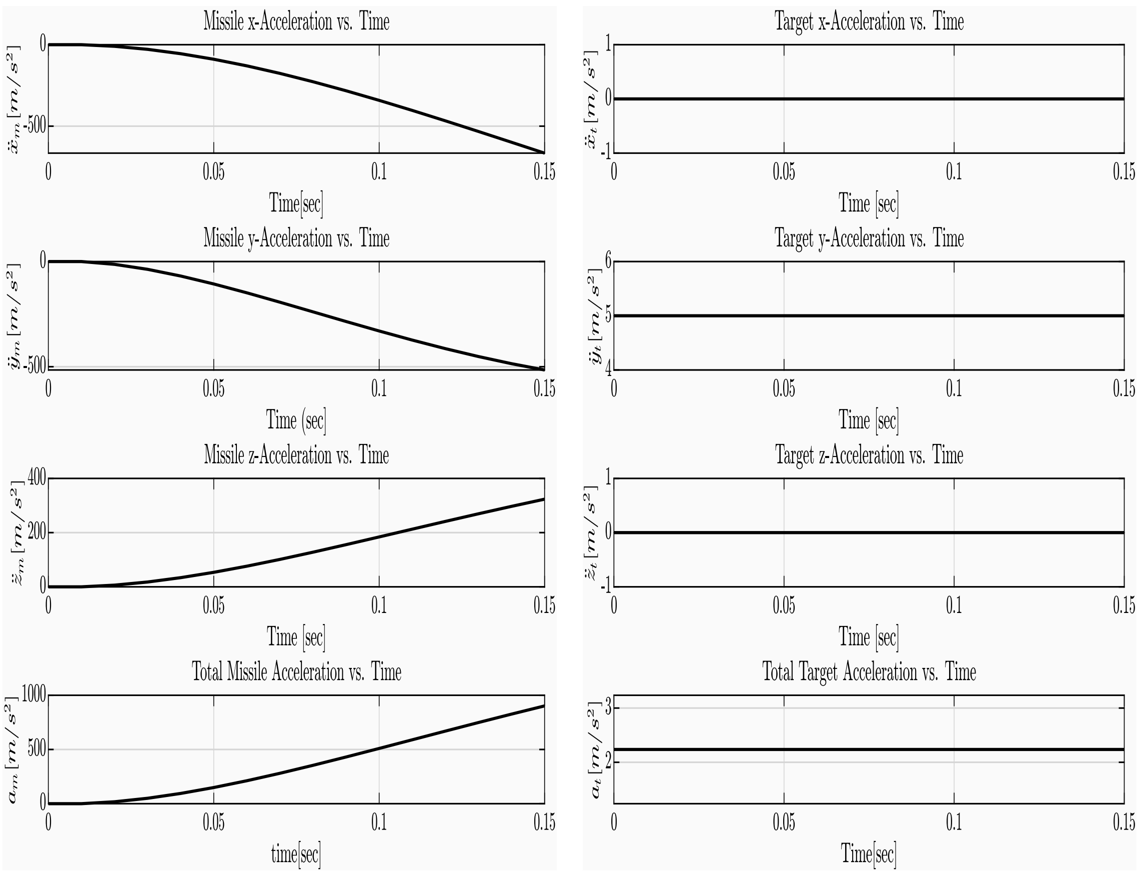
Missile x-Acceleration vs. Time
$\ddot{x}_m[m/s^2]$
Time[sec]
Target x-Acceleration vs. Time
$\ddot{x}_t[m/s^2]$
Time [sec]
Missile y-Acceleration vs. Time
$\ddot{y}_m[m/s^2]$
Time (sec)
Target y-Acceleration vs. Time
$\ddot{y}_t[m/s^2]$
Missile z-Acceleration vs. Time
$\ddot{z}_m[m/s^2]$
Target z-Acceleration vs. Time
$\ddot{z}_t[m/s^2]$
Total Missile Acceleration vs. Time
$a_m[m/s^2]$
time[sec]
Total Target Acceleration vs. Time
$a_t[m/s^2]$
Time[sec]

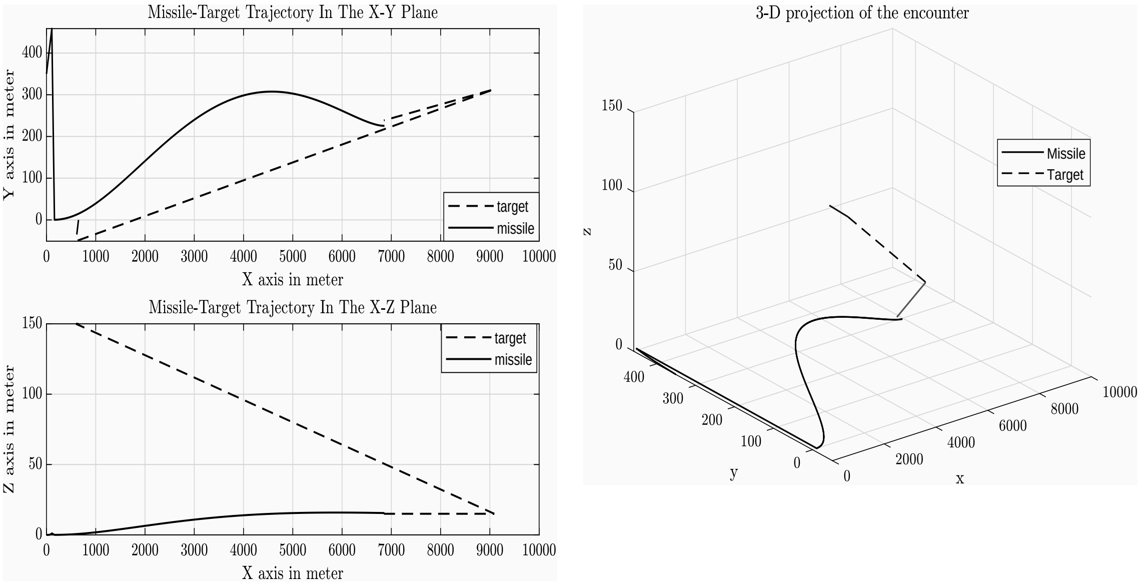

Figure 5.3: Constant acceleration target scenario

Scenario 3: A Three Dimensional Target Acceleration

The target performs three dimensional maneuver toward the missile and to the vertical at a range of $3,500m$. The target acceleration is

$$a_{xt} = -6.5 * 32.2 * sin(\gamma_{t\_pitch})$$

$$a_{yt} = 6.5 * 32.2 * cos(\gamma_{t\_yaw})$$

$$a_{zt} = 6.5 * 32.2 * cos(\gamma_{t\_pitch})$$

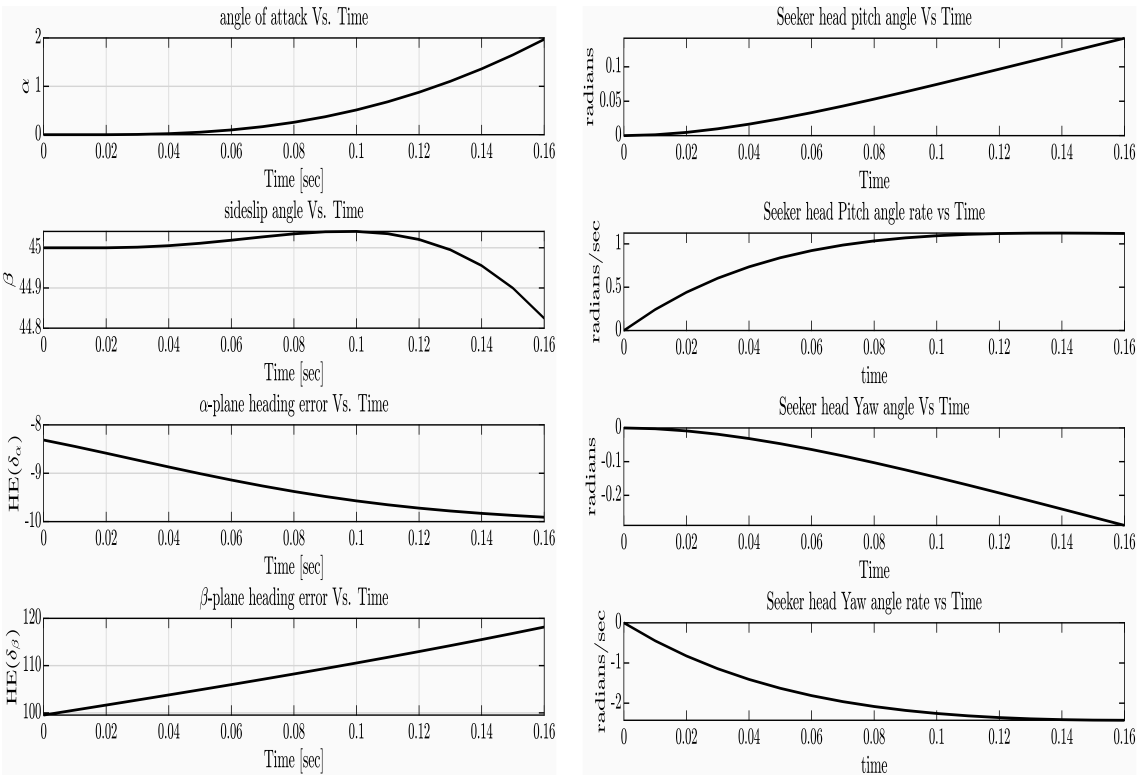

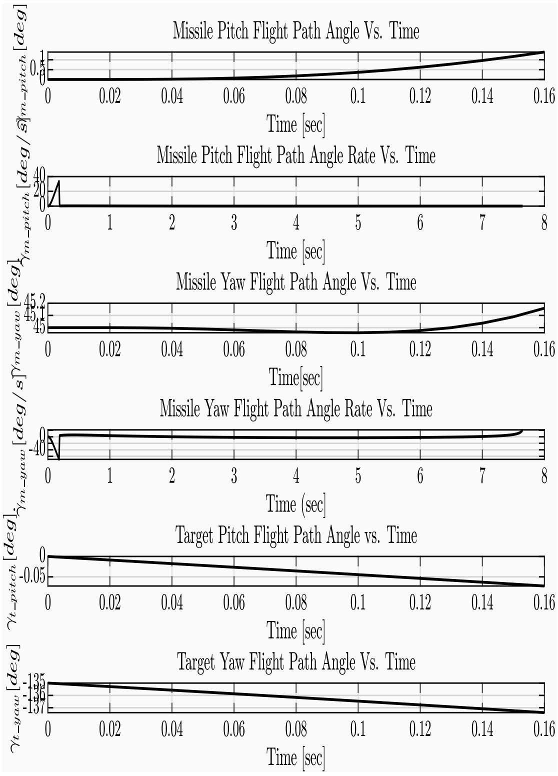
Missile Pitch Flight Path Angle Vs. Time
Time [sec]
Missile Pitch Flight Path Angle Rate Vs. Time
Time [sec]
Missile Yaw Flight Path Angle Vs. Time
Time[sec]
Missile Yaw Flight Path Angle Rate Vs. Time
Time (sec)
Target Pitch Flight Path Angle vs. Time
Time [sec]
Target Yaw Flight Path Angle Vs. Time
Time [sec]

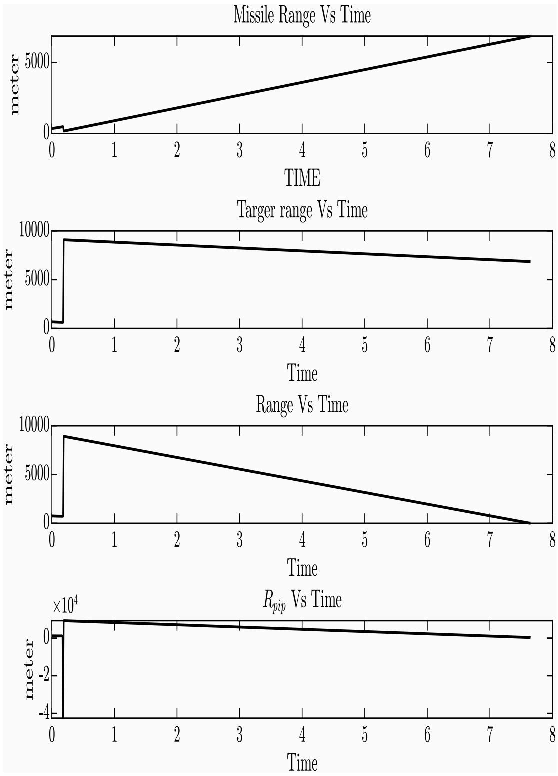
Missile Range Vs Time
meter
TIME
Targer range Vs Time
meter
Time
Range Vs Time
meter
Time
R_{pip} Vs Time
meter
Time

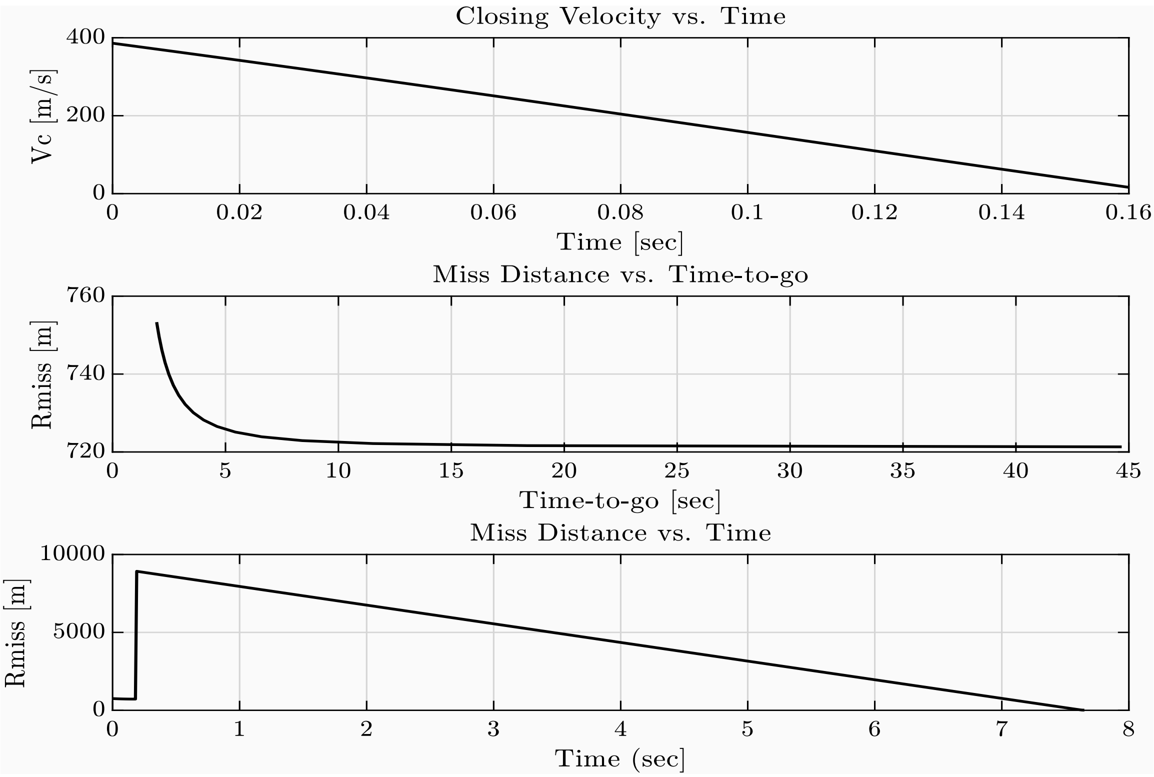
Closing Velocity vs. Time
Vc [m/s]
Time [sec]
Miss Distance vs. Time-to-go
Rmiss [m]
Time-to-go [sec]
Miss Distance vs. Time
Rmiss [m]
Time (sec)

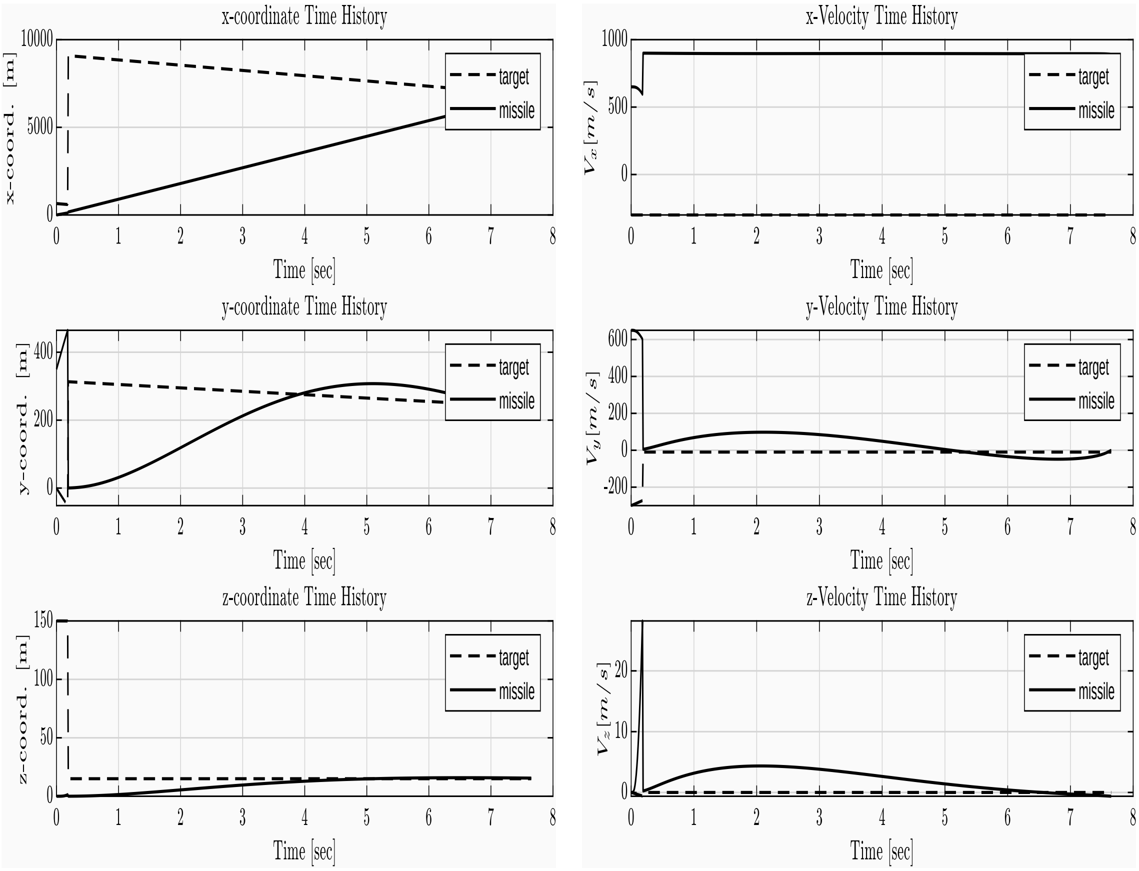

x-coordinate Time History
x-coord. [m]
Time [sec]
target
missile
x-Velocity Time History
$V_x[m/s]$
Time [sec]
target
missile
y-coordinate Time History
y-coord. [m]
Time [sec]
target
missile
y-Velocity Time History
$V_y[m/s]$
Time [sec]
target
missile
z-coordinate Time History
z-coord. [m]
Time [sec]
target
missile
z-Velocity Time History
$V_z[m/s]$
Time [sec]
target
missile

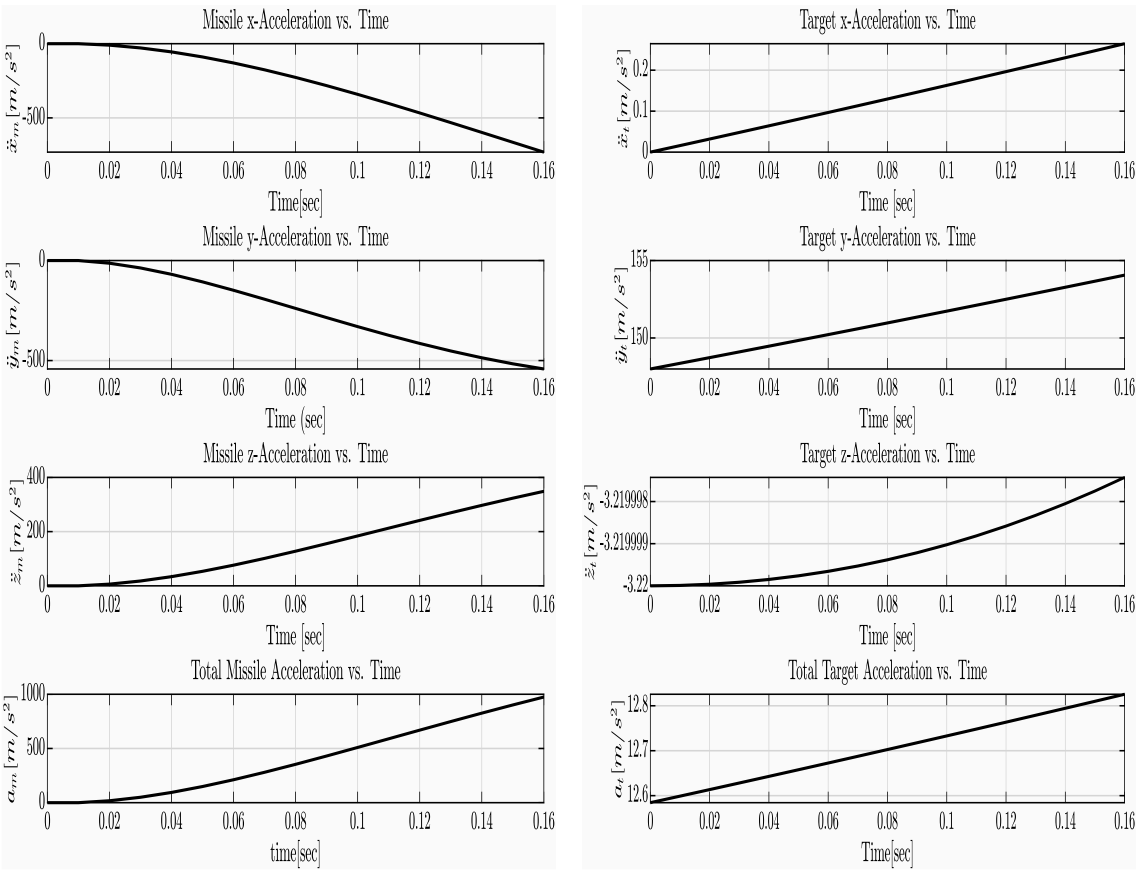

Missile x-Acceleration vs. Time
$\ddot{x}_m[m/s^2]$
Time[sec]
Target x-Acceleration vs. Time
$\ddot{x}_t[m/s^2]$
Time [sec]
Missile y-Acceleration vs. Time
$\ddot{y}_m[m/s^2]$
Time (sec)
Target y-Acceleration vs. Time
$\ddot{y}_t[m/s^2]$
Time (sec)
Missile z-Acceleration vs. Time
$\ddot{z}_m[m/s^2]$
Time [sec]
Target z-Acceleration vs. Time
$\ddot{z}_t[m/s^2]$
Time [sec]
Total Missile Acceleration vs. Time
$a_m[m/s^2]$
time[sec]
Total Target Acceleration vs. Time
$a_t[m/s^2]$
Time[sec]

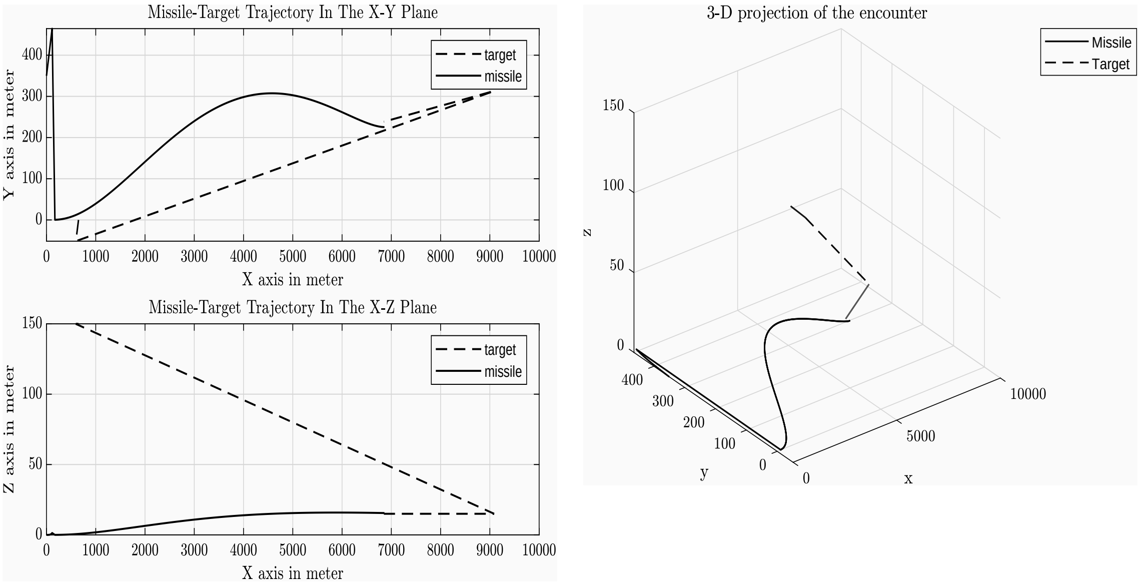

Figure 5.4: Three Dimensional Target Acceleration plots

In traditional missile guidance system the guidance law uses relative missile/target states to generate acceleration commands without any connection to the autopilot design. This proportional navigation guidance law is tested assuming functioning autopilot. As shown in the above scenarios proportional navigation is effective to achieve the hit-to-kill interception so, it is promising to transfer the objective of PN guidance law into designing fin deflection control inputs utilizing velocity based integrated guidance and control formulation.
Simulations are done using MATLAB.

Chapter 6

Conclusion and Recommendation

6.1 Conclusion

This thesis was originally started to solve general problems regarding guided missile system using sliding mode control. It was found that guided missiles have two subsystems which are Guidance and control(autopilot). The traditional approach for missile guidance and control is to design these subsystems separately due to the assumption that there is a spectral separation between guidance and control loops. If the overall system performance is unsatisfactory individual subsystems are redesigned to improve the whole system performance. But, traditional approach is proved to be inadequate when the target has strong maneuverability because the spectral separation assumption becomes invalid due to fast geometry changes. This leads to looks for a better approach which is integrated guidance and control(IGC). IGC approach exploits the synergy between guidance and control and these subsystems are executed in one single loop. There are two ways of formulating integrated guidance and control system which are body based formulation and velocity based formulation. Body based IGC formulation utilizes the missile body frame, but the problem with this formulation is that it cannot accurately capture the physics behind missile motion. So, velocity based IGC formulation which is based on missile velocity was chosen. It is shown that sliding mode control method is a preferable choice for the robustness to target acceleration uncertainty and steering the missile to target quickly. The more natural guidance parameter to be selected as sliding surface for velocity based IGC formulation was found to be heading error.
In this thesis, missile dynamics and missile-target engagement kinematics are developed. Theoretical analysis is done based on the previously developed velocity based integrated guidance and control formulation. Fin deflection control laws are derived using terminal sliding mode control as it is an efficient way to attenuate chattering. Finally, airframe simulation and missile target engagement simulation scenarios are shown using proportional navigation.

6.2 Recommendation

This thesis has the aim of showing the effectiveness of sliding mode control method for integrated guidance and control paradigm. Any other robust control methods can be applied and better guidance and control methods can be derived.

References

[1] S. Balakrishnan, A. Tsourdos, and B. A. White, *Advances in missile guidance, control, and estimation.* CRC Press, 2012.

[2] N. F. Palumbo, "Guest editors introduction: Homing missile guidance and control," *John Hopkins APL Technical Digest*, vol. 29, no. 1, pp. 2–8, 2010.

[3] P. H. Zipfel, *Modeling and simulation of aerospace vehicle dynamics.* American Institute of Aeronautics and Astronautics, 2007.

[4] B. of Naval Personnel, *Principles of Guided Missiles and Nuclear Weapons*, 1966.

[5] M. SPEARMAN, "Historical development of world wide guided missiles," in *16th Aerospace Sciences Meeting*, 1983, p. 210.

[6] P. Zarchan, *Tactical and strategic missile guidance.* American Institute of Aeronautics and Astronautics, Inc., 2012.

[7] R. Yanushevsky, *Modern missile guidance.* CRC Press, 2007.

[8] M. Kaushik and P. R. Hanmaiahgari, "Missiles," in *Essentials of Aircraft Armaments.* Springer, 2017, pp. 25–44.

[9] E. Ohlmeyer and P. Menon, "Nonlinear integrated guidance-control laws for homing missiles," in *AIAA Guidance, Navigation, and Control Conference and Exhibit*, 2001, p. 4160.

[10] N. F. Palumbo, B. E. Reardon, and R. A. Blauwkamp, "Integrated guidance and control for homing missiles," *Johns Hopkins APL Technical Digest*, vol. 25, no. 2, pp. 121–139, 2004.

[11] Z. Fu, Y. Dai, and K. Zhang, "Research progress on design methods for missile integrated guidance and control," in *Proceedings of the 2017 International Conference on Automation, Control and Robots.* ACM, 2017, pp. 15–19.

[12] T. Yamasaki, S. Balakrishnan, and H. Takano, "Integrated guidance and autopilot design for a chasing uav via high-order sliding modes," *Journal of the Franklin Institute*, vol. 349, no. 2, pp. 531–558, 2012.

[13] R. Padhi, C. Chawla, and P. G. Das, "Partial integrated guidance and control of interceptors for high-speed ballistic targets," *Journal of Guidance, Control, and Dynamics*, vol. 37, no. 1, pp. 149–163, 2013.

[14] I. Shkolnikov, Y. Shtessel, and D. Lianos, "Integrated guidance-control system of a homing interceptor- sliding mode approach," in *AIAA Guidance, Navigation, and Control Conference and Exhibit, Montreal, Canada*, 2001.

[15] T. Shima, M. Idan, and O. M. Golan, "Sliding-mode control for integrated missile autopilot guidance," *Journal of guidance, control, and dynamics*, vol. 29, no. 2, pp. 250–260, 2006.

[16] A. A. A. Alrawi, S. Graovac, R. B. Ahmad, M. Rahman *et al.*, "Modified guidance law based on a sliding mode controller for a missile guidance system," *Tehnički vjesnik*, vol. 23, no. 3, pp. 639–646, 2016.

[17] M. Dancer, S. Balakrishnan, and E. Ohlmeyer, "Discussion and analysis of missile igc design," in *AIAA guidance, navigation and control conference and exhibit*, 2008, p. 7002.

[18] F. A. Faruqi and T. L. Vu, "Mathematical models for a missile autopilot design," DEFENCE SCIENCE AND TECHNOLOGY ORGANISATION CANBERRA (AUSTRALIA), Tech. Rep., 2002.

[19] F. C. Lukenbill, "A target/missile engagement scenario using classical proportional navigation," NAVAL POSTGRADUATE SCHOOL MONTEREY CA, Tech. Rep., 1990.

[20] N. Harl, S. Balakrishnan, and C. Phillips, "Sliding mode integrated missile guidance and control," in *AIAA guidance, navigation, and control conference*, 2010, p. 7741.

[21] C. Edwards and S. Spurgeon, *Sliding mode control: theory and applications.* Crc Press, 1998.

[22] V. Utkin, J. Guldner, and J. Shi, *Sliding mode control in electro-mechanical systems.* CRC press, 2009.

[23] A. Levant, "Sliding order and sliding accuracy in sliding mode control," *International journal of control*, vol. 58, no. 6, pp. 1247–1263, 1993.

[24] J.-J. E. Slotine, W. Li *et al.*, *Applied nonlinear control.* Prentice hall Englewood Cliffs, NJ, 1991, vol. 199, no. 1.

[25] Y. Shtessel, C. Edwards, L. Fridman, and A. Levant, *Sliding mode control and observation.* Springer, 2014.

[26] L. M. Capisani, A. Ferrara, and L. Magnani, "Design and experimental validation of a second-order sliding-mode motion controller for robot manipulators," *International Journal of Control*, vol. 82, no. 2, pp. 365–377, 2009.

[27] N. Harl and S. Balakrishnan, "Reentry terminal guidance through sliding mode control," *Journal of guidance, control, and dynamics*, vol. 33, no. 1, pp. 186–199, 2010.

[28] J. Yu, D. Tang, W.-j. Gu, and Q. Xu, "The application of tsm control to integrated guidance/autopilot design for missiles," in *International Conference on Intelligent Computing.* Springer, 2005, pp. 326–335.

[29] Z. Jialing and Y. Jianying, "Integrated missile guidance and control design with smooth adaptive sliding mode control," in *2015 34th Chinese Control Conference (CCC).* IEEE, 2015, pp. 5206–5211.

Appendices

A Proof of the Result in Theorem 1

The proof is shown in[27]. Assume that a sliding surface is chosen as

$$s = f(x) = 0 \tag{A1}$$

and that the first two time derivatives of the surface (A1) are

$$\dot{s} = h(x) \tag{A2}$$

$$\ddot{s} = l(x) + g(x)u \tag{A3}$$

Consider the control law

$$\dot{s} = -\frac{ns}{t_r - t} \tag{A4}$$

where t_r is the desired reaching time for the sliding surface in equation (A1). The control law in equation (A4) specifies a constraint on the sliding surface derivative that will not necessarily be satisfied at the initial time. A second-order sliding mode control law can be found such that the constraint (A4) can be met in some finite time t_r^*, which is less than t_r. Now assume that at the time t_r^*, the sliding surface of equation (A1) is equal to some finite value s^*. At that point, the system (A1-A3) satisfies the constraint in equation (A4). Rearranging variables, equation (A4) can be rewritten as

$$\frac{ds}{s} = -n\frac{dt}{t_r - t} \tag{A5}$$

Now equation (A5) can be integrated from the point (s^*, t_r^*) to some later point (s, t), yielding

$$\ln\left(\frac{s}{s^*}\right) = n\ln\left(\frac{t_r - t}{t_r - t_r^*}\right) = \ln\left[\left(\frac{t_r - t}{t_r - t_r^*}\right)^n\right] \tag{A6}$$

Taking the exponential of both sides of equation (A6), an analytic equation for s can be found as

$$s = \frac{s^*}{(t_r - t_r^*)^n}(t_r - t)^n = \Psi(t_r - t)^n \tag{A7}$$

where β is a constant

$$\Psi = \frac{s^*}{(t_r - t_r^*)^n} \tag{A8}$$

Finally, differentiating equation (A7), an analytic equation for $\dot{s}$ can be found as

$$\dot{s} = -n\Psi(t_r - t)^{n-1} \tag{A9}$$

Equations (A7) and (A9) are analytic expressions for the sliding surface and its derivative after the finite time t_r^* has been reached. Now, inspecting these equations, it can be seen that s and $\dot{s}$ will have a certain behavior as the time t approaches the reaching time t_r depending on the value chosen for n. First, it can be seen from equation (A7) that as long as n is greater than zero, the sliding surface will go to zero at the desired reaching time. The primary dependence on n is seen when analyzing the behavior of $\dot{s}$. If n is less than one, equation (A9) exhibits a singularity as the reaching time is approached, an obviously undesired result. By setting n equal to one, it can be seen that $\dot{s}$ no longer exhibits a singularity, but instead converges to a constant (Ψ). For this value of n, the system (A1-A3) would exhibit a behavior that is characteristic to a traditional first-order sliding mode control law. If n is set to be greater than one, equation (A9) shows that the flight-path angle will go to zero as the reaching time is approached. Thus, as long as n is selected to be greater than one, it can be guaranteed that the sliding surface and its derivative will go to zero at the desired reaching time.

B MATLAB Snippets

MATLAB code for calculation of flight parameters

```
runtime = clock;
rtod = 180/pi;

% Initialization
ms(:,1) = [0;650;350;650;0;0];
ts(:,1) =  [650; 300;0; 300;150;0];
trks(:,1) = [0;0;0;0];
mc(:,1) = [0;0];
nc(:,1) = [0;0];
Rt(1) = sqrt(ts(1,1)^2 + ts(3,1)^2 + ts (5,1)^2);
Rm(1) = sqrt(ms(1,1)^2 + ms(3,1)^2 + ms (5,1)^2);
R(1) = sqrt((ms(1,1)  ts(1,1))^2+(ms(3,1)  ts(3,1))^2+(ms(5,1)  ts(5,1))^2);
R_pitch(1) = sqrt((ms(1,1)  ts(1,1))^2+(ms(5,1)  ts(5,1))^2);
R_yaw(1) = sqrt((ms(1,1)  ts(1,1))^2+(ms(3,1)  ts(3,1))^2);
time(1) = 0;

xt = ts(1,1);
yt = ts(3,1);
zt = ts(5,1);

xdt = ts(2,1);
ydt = ts(4,1);
zdt = ts(6,1);

xm = ms(1,1);
ym = ms(3,1);
zm = ms(5,1);

```

```
xdm = ms(2,1);
ydm = ms(4,1);
zdm = ms(6,1);

phiT = 30;
phiM = 20;

m = 400;
Iyy = 136;
g = 9.81;
rhorho = 0.2641;
s = 10;
knb(1) = 1;
kyb(1) = 1;
knd(1) = 1;
kNa(1) = 2;
kma(1) = 2;
kmd(1) = 2000;
q(1) = 2;
HE_pitch(1) = 20;
HE_yaw(1) = 30;
qd(1) = 1000;
del_pitch(1) = 0;
alf_d(1) = 0;

n = 3;
eta = 2;
ro1 = 0;
ro2 = 0;

AM = [0 1 0 0 0 0
      0 0 0 0 0 0
      0 0 0 1 0 0
      0 0 0 0 0 0
      0 0 0 0 0 1
      0 0 0 0 0 0];

BM = [0 0 0
      1 0 0
      0 0 0
      0 1 0
      0 0 0
      0 0 1];

AT = AM;
BT = BM;

ttrack = 0.1;
```

```
tmc = 1;
N = 4;
k1 = (1/ttrack)^2;
k2 = (2/ttrack);
k = (1/tmc);

ATR = [   0    1   0    0
          k1   k2  0    0
          0    0   0    1
          0    0   k1   k2];

BTR = [  0   0
         k1  0
         0   0
         0  k1];

 AMC = [ k  0
         0   k];
 BMC = [N  0
         0  N];

% Discretization
dt = 0.01;
[phim,delm] = c2d(AM,BM,dt);
[phit,delt] = c2d(AT,BT,dt);
[phitr,deltr] = c2d(ATR,BTR,dt);
[phimc,delmc] = c2d(AMC,BMC,dt);

tfinal = 15.0;
kmax = tfinal/dt+1;

for i=1:kmax 1
% Missile and Target Velocities
vt(i) = sqrt(ts(2,i)^2 + ts(4,i)^2 + ts(6,i)^2);
vm(i) = sqrt(ms(2,i)^2 + ms(4,i)^2 + ms(6,i)^2);
vt_pitch(i) = sqrt(ts(2,i)^2+ts(6,i)^2);

% Lines of sight angles
sigmam_pitch(i) = atan2(ms(5,i),sqrt (ms(1,i)^2+ms(3,i)^2));
sigmat_pitch(i) = atan2(ts(5,i),sqrt (ts(1,i)^2+ts(3,i)^2));
sigmam_yaw(i) = atan2(ms(3,i),ms(1,i));
sigmat_yaw(i) = atan2(ts(3,i),ts(1,i));
sigma_pitch(i) = atan2((ts(5,i) ms(5,i)),sqrt((ts(1,i)^2 ms
    (1,i)^2)+(ts(3,i)^2 ms(3,i)^2)));
sigma_yaw(i) = atan2((ts(3,i) ms(3,i)),(ts(1,i) ms(1,i)));
utr = [sigma_pitch(i)
         sigma_yaw(i)   ];

```

```
%angle of attack and sideslip angle
 alf(i) = atan2(ms(6,i),ms(2,i));
 bet(i) = asin(ms(2,i)/vm(i));

% F.C.S. Missile Command Control update
umc(:,i) = [trks(2,i)
            trks(4,i)];

% Missile and Target Flight Path angles
gammam_pitch(i) = atan2(ms(6,i),sqrt(ms(2,i)^2+ms(4,i)^2));
gammat_pitch(i) = atan2(ts(6,i),sqrt(ts(2,i)^2+ts(4,i)^2));
gammam_yaw(i) = atan2(ms(4,i),ms(2,i));
gammat_yaw(i) = atan2(ts(4,i),ts(2,i));

% heading error in each plane
  gammamd_pitch(i) = sigma_pitch(i) + asin((vt(i)/vm(i))*sin(
     gammat_pitch(i) sigma_pitch(i)));
  HE_pitch(i) = gammam_pitch(i) gammamd_pitch(i);
  gammamd_yaw(i) = sigma_yaw(i) + asin((vt(i)/vm(i))*sin(
     gammat_yaw(i) sigma_yaw(i)));
  HE_yaw(i) = gammam_yaw(i) gammamd_yaw(i);

% F.C.S. Tracker update
trks(:,i+1) = phitr*trks (:,i) + deltr*utr;

% F.C.S. Missile Command update
mc(:,i+1) = phimc*mc(:,i)+delmc*umc(:,i);

% Missile Velocity and Acceleration in Pitch Plane
vm_pitch(i) = vm(i)*cos(gammam_yaw(i) sigmam_yaw(i));
am_pitch(i) = vm_pitch(i)*mc(1,i);

% Missile Pitch Acceleration components
xddm_pitch(i) =  am_pitch(i)*sin(sigma_pitch(i))*cos (
    sigma_yaw(i));
yddm_pitch(i) =  am_pitch(i)*sin(sigma_pitch(i))*sin (
    sigma_yaw (i));
zddm_pitch(i) = am_pitch(i)*cos(sigma_pitch(i));

% Missile Velocity and Acceleration in Yaw Plane
vm_yaw(i) = vm(i)*cos(gammam_pitch(i));
am_yaw(i) = vm_yaw(i)*mc(2,i);

% Missile Yaw Acceleration components
xddm_yaw(i) =  am_yaw(i)*sin(sigma_yaw(i));
yddm_yaw(i) = am_yaw(i)*cos(sigma_yaw(i));
```

```
% Missile Acceleration components
xddm(i) = xddm_pitch(i)+xddm_yaw(i);
yddm(i) = yddm_pitch(i)+yddm_yaw(i);
zddm(i) = zddm_pitch(i);
um = [xddm(i)
      yddm(i)
      zddm(i)];
am(i) = sqrt(um(1)^2+um(2)^2+um(3)^2);

% Missile update
ms(:,i+1) = phim*ms(:,i)+delm*um;

% Target Acceleration components
% xddt(i) = 0;
% yddt(i) = 0;
% zddt(i) = 0;
xddt(i) =  6.5*32.2*sin(gammat_pitch(i));
yddt(i) =  6.5*32.2*cos(gammat_yaw(i));
zddt(i) =  0.1*32.2*cos(gammat_pitch(i));
ut = [xddt(i)
      yddt(i)
      zddt(i)];
at(i) = sqrt(ut(1)^2+ut(2)+ut(3)^2);
at_pitch(i) = sqrt(ut(1)^2+ut(3)^2);

% Target update
ts (:,i+1) = phit*ts (:,i) + delt*ut;

% Time to go
vt_yaw(i) = vt(i)*cos(gammat_pitch(i));
vc(i) =  (vt_yaw(i)*cos(gammat_yaw(i) sigma_yaw(i)) vm_yaw(i)*cos(gammam_yaw(i) sigma_yaw(i)));
t_go(i) = R(i)/vc(i);

% PIP location
% distances in alpha and beta plane
R_alph(i) = sqrt((ts(1,i) ms(1,i))^2+(ts(5,i) ms(5,i))^2); % x z plane
R_beta(i) = sqrt((ts(1,i) ms(1,i))^2+(ts(3,i) ms(3,i))^2); % x y plane
R_pip(i) = R(i)+vt(i)+t_go(i);
R_pip_pitch(i) = R_alph(i) + vt_pitch(i)*t_go(i);
v_rel(i) = vt_pitch(i)   vm_pitch(i);
R_pipd(i) = at(i)*t_go(i) (vt(i)*(R_pip(i) Rm(i))*at(i)*t_go(i))/((R_pip(i) Rm(i))*v_rel(i));

% pitch and yaw fin deflections
KNa(i) =  (rhorho*vm_pitch(i)*s)/(2*m);
```

```
A(i) = (xt xm + t_go(i)*xdt)*t_go(i)*sin(gammat_pitch(i)) (zt zm + t_go(i)*zdt)*t_go(i)*cos(gammat_pitch(i));
B(i) = (xt xm + t_go(i)*xdt)*t_go(i)*sin(phiT) (yt ym + t_go(i)*ydt)*t_go(i)*cos(phiT);
C(i) = (xt xm + xdt*t_go(i))*(xdt xdm) + (yt ym + ydt*t_go(i))*(ydt ydm) + (zt zm + zdt*t_go(i))*(zdt zdm);
D(i) = ( t_go(i)*sin(gammat_pitch(i)) + (A(i)/C(i))*xdt)*sin(gammam_pitch(i) HE_pitch(i)) (t_go(i)*cos(gammat_pitch(i)) + (A(i)/C(i))*zdt)*cos(gammam_pitch(i) HE_pitch(i));
E(i) = ( t_go(i)*sin(phiT) + (B(i)/C(i))*xdt)*sin(gammam_pitch(i) HE_pitch(i)) (B(i)/C(i))*zdt*cos(gammam_pitch(i) HE_pitch(i));
 HEd_pitch(i) = (vm_pitch(i)/R_alph(i))*sin(HE_pitch(i))+kNa*alf(i)+(D(i)/R_alph(i))*at_pitch(i)+(E(i)/R(i))*at_pitch(i);
 HEdd_pitch(i) = (vm_pitch(i)/R_alph(i))^2*sin(2*HE_pitch(i)) + (vm(i)/R_alph(i))*cos(HE_pitch(i))*kNa*alf(i)+kNa*(trks(2,1) kNa*alf(i))+ro1;

 I = kNa*kmd;
H(i) = 2*(vm_pitch(i)/R(i))^3*sin(3*HE_pitch(i)) + 3*(vm_pitch(i)/R(i))^2*cos(2*HE_pitch(i))*kNa*alf(i) (vm_pitch(i)/R(i))*sin(HE_pitch(i))*(kNa*alf(i))^2+...
         (vm_pitch(i)/R(i))*cos(HE_pitch(i))*kNa*( kNa*alf(i)+trks(2,1))+kNa*( kNa*( kNa*alf(i)+trks(2,1))+kma*alf(i));
 del_pitch(i) = ( 1/I)*(H(i) +(2*n*HEdd_pitch(i)*t_go(i)^2 + n*(n+3)*HEd_pitch(i)*t_go(i)+2*n*(n+1)*HE_pitch(i))/t_go(i)^3 + ...
                  (eta+abs(ro2))*sign((HEdd_pitch(i)*t_go(i)^2 + 2*n*HEd_pitch(i)*t_go(i) + n*(n+1)*HE_pitch(i))/t_go(i)^2));
 HEddd_pitch(i) = 2*(vm_pitch(i)/R(i))^3*sin(3*HE_pitch(i)) + 3*(vm_pitch(i)/R(i))^2*cos(2*HE_pitch(i))*kNa*alf(i) (vm_pitch(i)/R(i))*sin(HE_pitch(i))*(kNa*alf(i))^2+...
         (vm_pitch(i)/R(i))*cos(HE_pitch(i))*kNa*( kNa*alf(i)+trks(2,1))+kNa*(kma*alf(i)+kmd*del_pitch(i) kNa*(trks(2,1) kNa*alf(i)))+ro2;

%derivatives of angle of attack and pitch rate
        q(i+1) = q(i) + dt*qd(i);
        qd(i+1) = kma*alf(i)+kmd*del_pitch(i);
        alf(i+1) = alf(i) +dt*alf_d(i);
        alf_d(i+1) =  kNa*alf(i) + q(i);

%command update
% nc(:,i+1) = del_pitch(i)+phimc*mc(:,i)+delmc*umc(:,i);
% vm_pitch(i+1) = vm(i)*cos(gammam_yaw(i) sigmam_yaw(i));
```

```
% am_pitch(i+1) = vm_pitch(i+1)*nc(1,i+1);

% Range update
Rt(i+1) = sqrt(ts(1,i+1)^2+ts(3,i+1)^2+ts(5,i+1)^2);
Rm(i+1) = sqrt(ms(1,i+1)^2+ms(3,i+1)^2+ms(5,i+1)^2);
R(i+1) = sqrt((ms(1,i+1) ts(1,i+1))^2+(ms(3,i+1) ts(3,i+1))^2+(ms(5,i+1) ts(5,i+1))^2);
R_pip(i+1) = R(i+1) + vt(i)*t_go(i);
v_rel(i+1) = vt(i)   vm(i);
R_pipd(i+1) = at(i)*t_go(i) (vt(i)*(R_pip(i+1) Rm(i+1))*at(i)*t_go(i))/((R_pip(i+1) Rm(i+1))*v_rel(i+1));
time(i+1) = time(i)+dt;

% Rmiss check
if (R(i) < R(i+1))
     tcpa = time(i);
    break
end
end
```